Used Fuel Disposition Campaign

THMC modeling and tests for EBS and clay host rock including thermal limits testing

Jonny Rutqvist, Liange Zhen, Fei Chen, HH Liu, Seiji Nakagawa, Timothy Kneafsey, Jens Birkholzer, Stefan Finsterle, Jonathan Ajo-Franklin

Lawrence Berkeley National Laboratory

Teleconference

January 10, 2013

THM Modeling Approach

TOUGH-FLAC

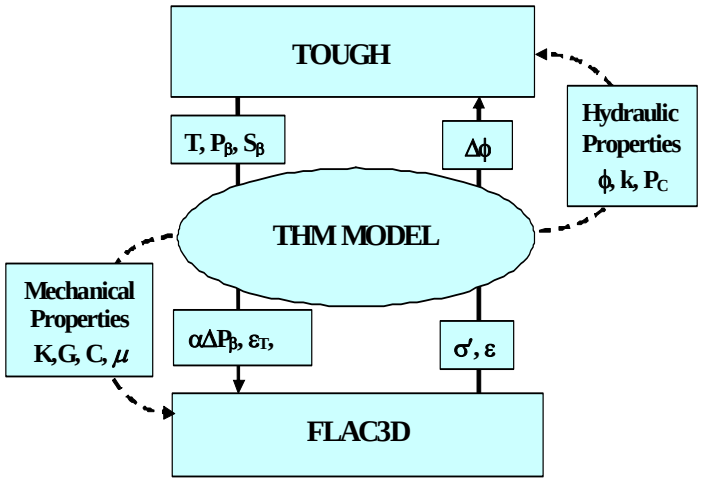

Numerical simulator for modeling coupled thermo-hydro-mechanical processes

Sequential coupling of TOUGH2 multiphase flow and heat transport simulator with FLAC3D geomechanical simulator

Barcelona Basic Model (BBM)

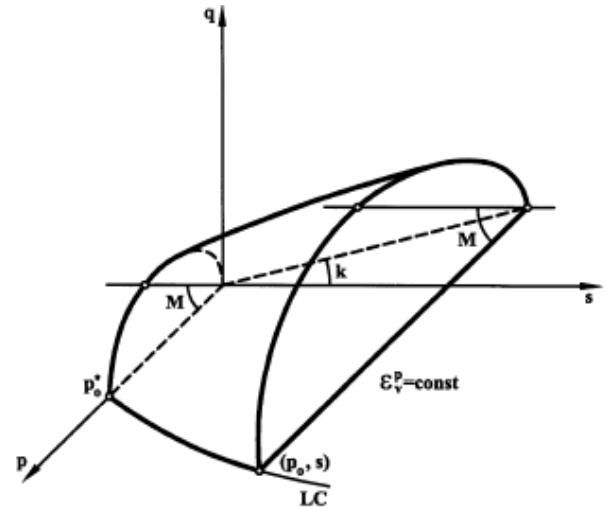

Constitutive model for thermo-elasto-plastic behavior of unsaturated soils

- Wetting-induced swelling or collapse strains
- Shear strength vs suction
- Preconsolidation stress vs suction.

FY2012 Accomplishments

- **Application of TOUGH-FLAC with BBM (Barcelona Basic Model) for modeling of coupled THM (thermal-hydrological-mechanical) processes in EBS**
- **THMC in TOUGHREACT-FLAC with secondary swelling is caused by changes in ionic concentration, which in turn is evaluated using a reactive transport simulation model.**
- **Implementation of double-structure model into TOUGH-FLAC (Barcelona Expansive Model)**
- **The two-part Hooke's model (TPHM) was implemented into the TOUGH-FLAC code and tested against data from the Mine-by Test at Mont Terri URL.**

Repository Model

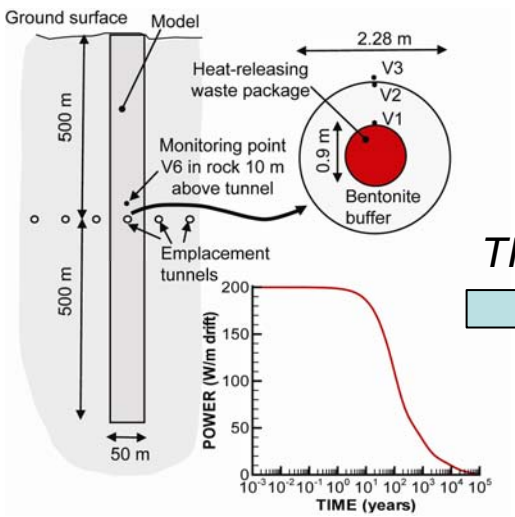

THMC

Flow and Transport

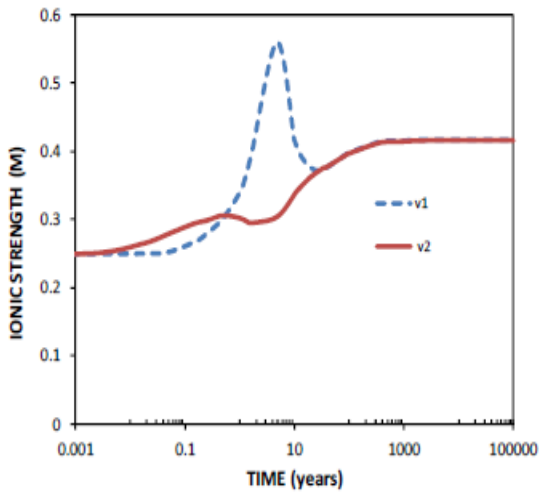

Buffer Swelling and Stress

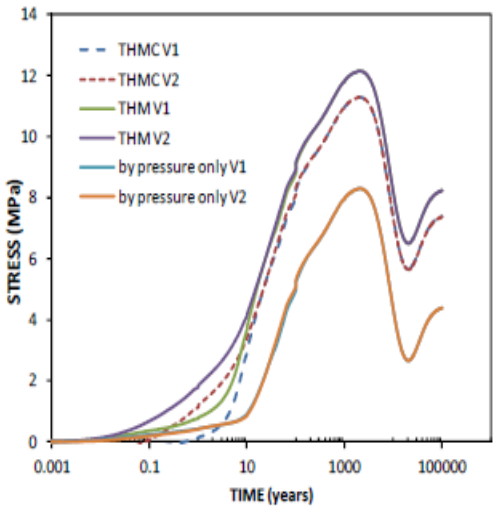

- **Results shows strong THMC interaction between EBS and host rock (e.g. thermal pressurization in host rock affects stress evolution in the buffer)**

THMC Model Developments

- **Extension of TOUGH-FLAC with BBM to TOUGHREACT-FLAC with Barcelona Expansive Model (BExM) that considers micro and macro structural interactions**
- **Serves as a framework for further extension to coupled THMC behavior (i.e., adding coupling to chemistry)**

CM coupling through 1) diffuse double layers theory or 2) as a function of ionic concentration

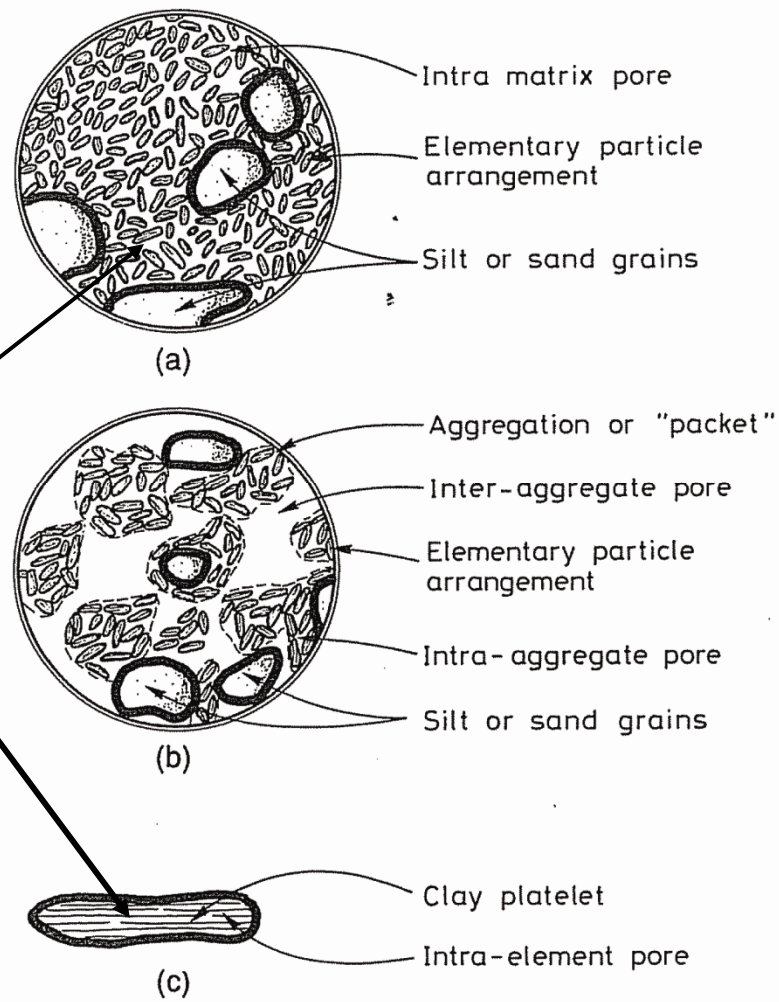

Used
Fuel
Disposition

THMC Model Development

Developing chemical-mechanical Coupling Constitutive Relationship: Two Ways of Coupling BExM to Chemistry .

Extension of TOUGH-FLAC-BBM to Barcelona Expansive Model (BExM) that considers micro and macro structural interactions (ongoing)

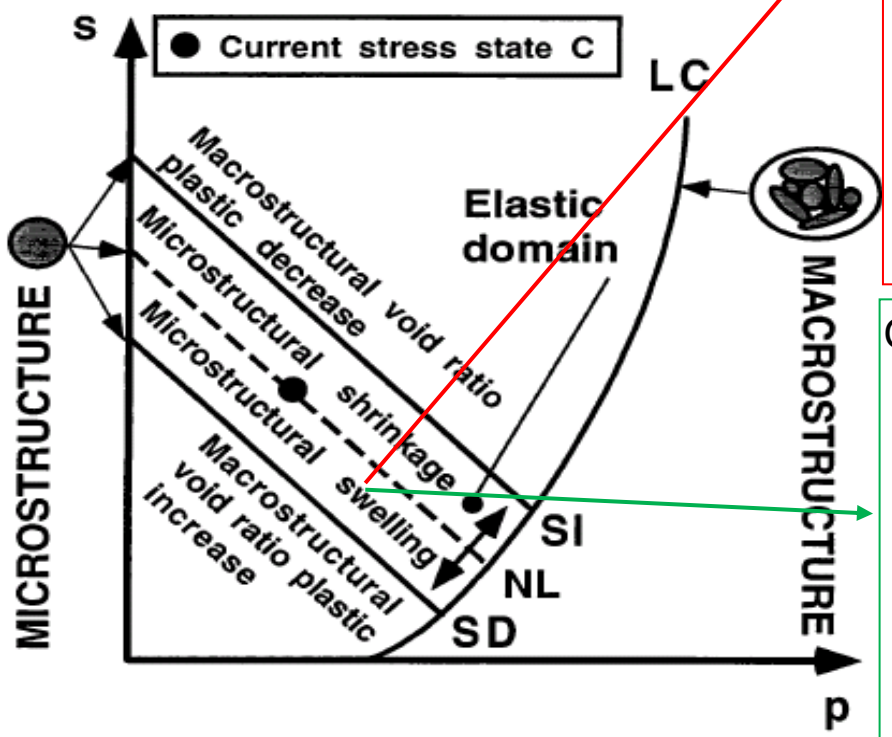

CM coupling through diffuse double layers theory: The microstructural swelling in the BExM is essentially the swelling in the interlayer space where a diffuse double layer exists.

Pros: allow us to consider the effect of the change of ion concentration, abundance of swelling minerals on the swelling.

Cons: the effect of exchangeable cations is taken into account through the weighted average of the valence of exchangeable cations rather than the concentration of each exchangeable cation.

CM coupling through the equations of Gens (2010):

$$d\varepsilon_m^e = \beta_m e^{-\alpha_m \hat{p}} d\hat{p} \qquad \beta_m = \sum_i \beta_m^i x_i$$

Pros: allow us to consider the effect of the change of ion concentration, the concentration of each exchangeable cation on the swelling.

Cons: the effect of the change of abundance of swelling minerals on the swelling is not considered.

Testing and Validation of THM and THMC models at Mont Terri Experiments

Major current or soon-to-be started experiments

HE-E Heater Test:

- *Focus on THM effects, bentonite rock interaction, seal and clay barrier performance*
- *Micro-tunnel*
- *Monitoring starts in Spring 2011*
- *Same location as previous ventilation experiment*

MB (Mine-by) Test:

- *Focus on HM effects, EDZ evolution*
- *Full-scale tunnel*
- *Monitoring phase completed*

FE Heater Test:

- *Focus on THM effects, validation of various bentonite/clay performance processes*
- *Full-scale tunnel*
- *Monitoring starts in Spring 2012*

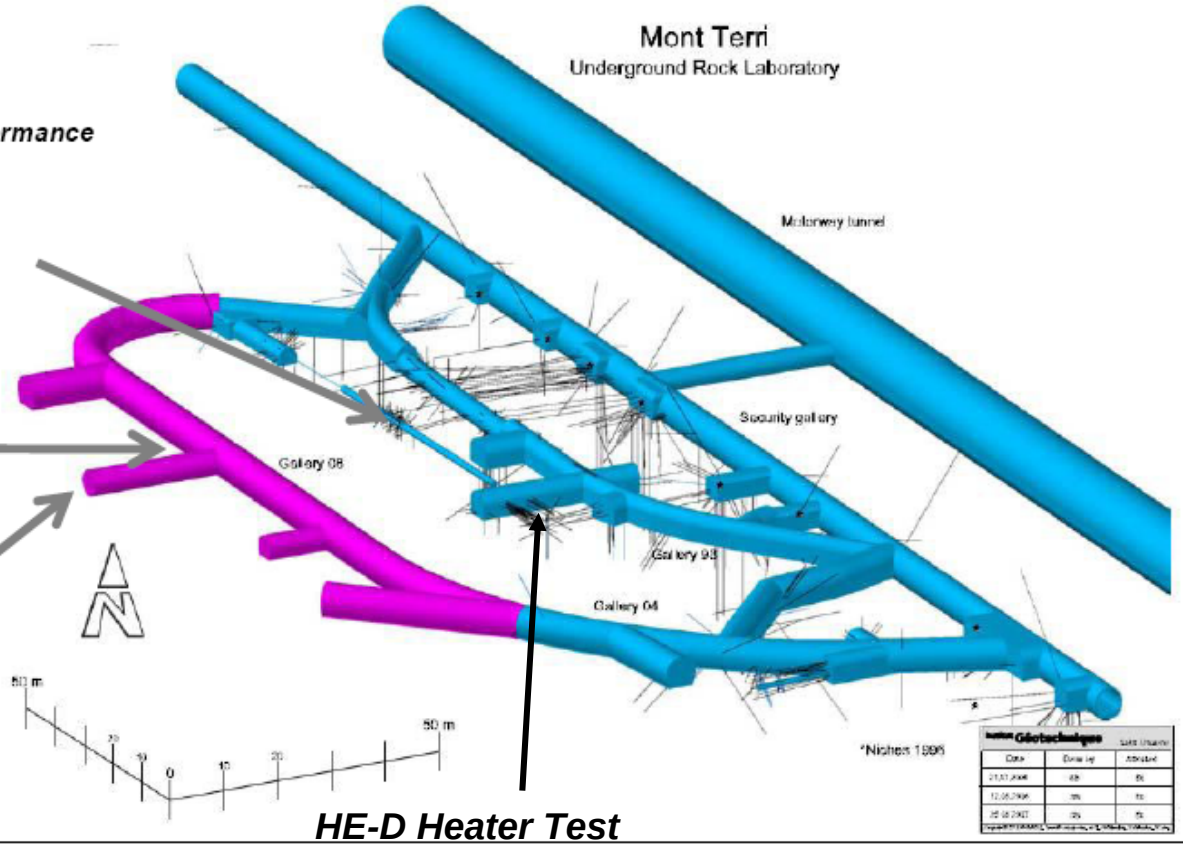

HE-D Heater Test

- ***THM effects in Opalinus Clay***
- ***Two heaters in a borhole***
- ***Heating March 2004 to June 2005***

Mont Terri HE Test Modeling

- 1st task is modeling previous Mont Terri rock mass HE-D heater test for calibration of THM rock properties
- Opalinus Clay thermal properties (anisotropic) back-calculated and thermal pressurization validated
- Anisotropic mechanical strength considering bedding planes as weak planes
- First results in LBNL/NAGRA paper for IHLWM conference 2013

Plane view of HE-D test at Mont Terri

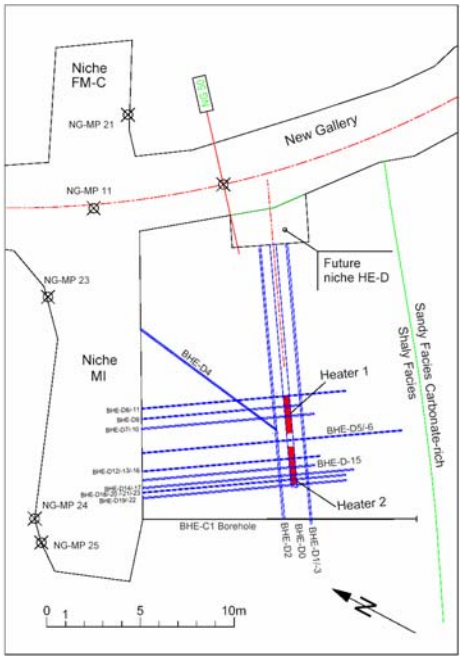

3D TOUGH-FLAC model

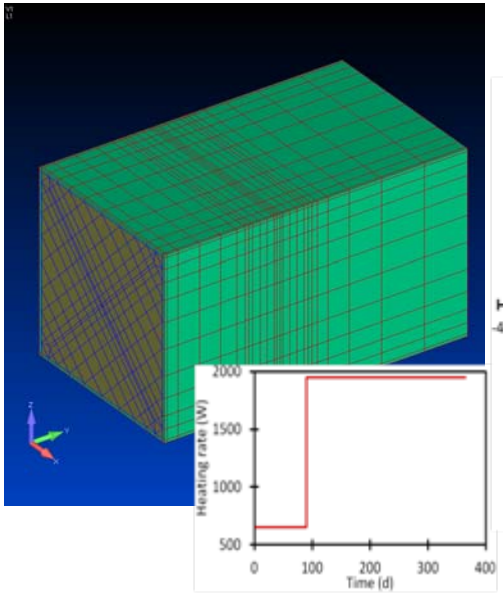

Vertical cross-section showing sensor locations

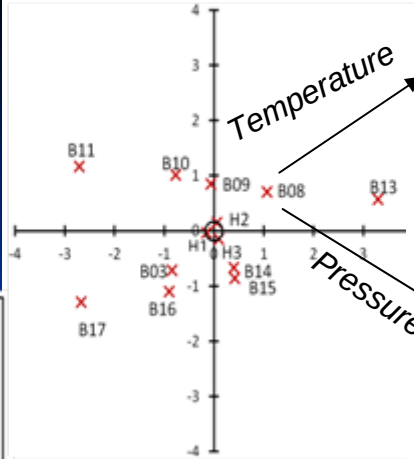

Simulated vs observed

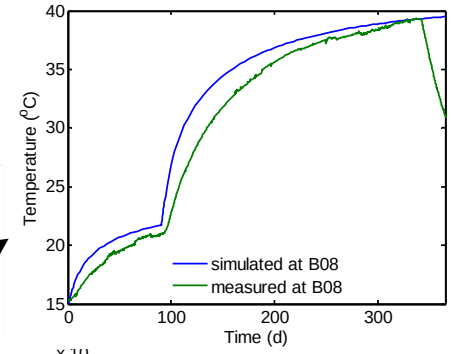

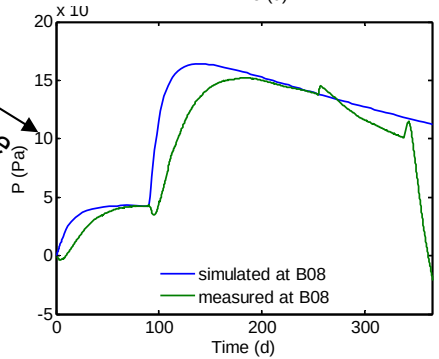

Mont Terri HE Test Modeling

FY13 Plan

- 3rd DECOVALEX 2015 Workshop to be held in Korea, April 15-19, 2013
- Buffer material study of THM experimental data provided by DECOVALEX to determine and calibrated buffer properties (until October 2013)
- Develop 3D TOUGH-FLAC THM model of HE test

Laboratory Experiment for buffer material study (example)

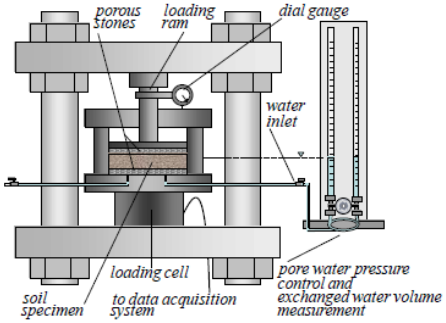

Figure 3.18 – Confined swelling test device: schematic cross section and picture of the cell used. The piston of the cell is designed in order to avoid bentonite leaking and to permit a good measurement of the swelling pressure.

(Rizzi et al 2012)

HE test layout

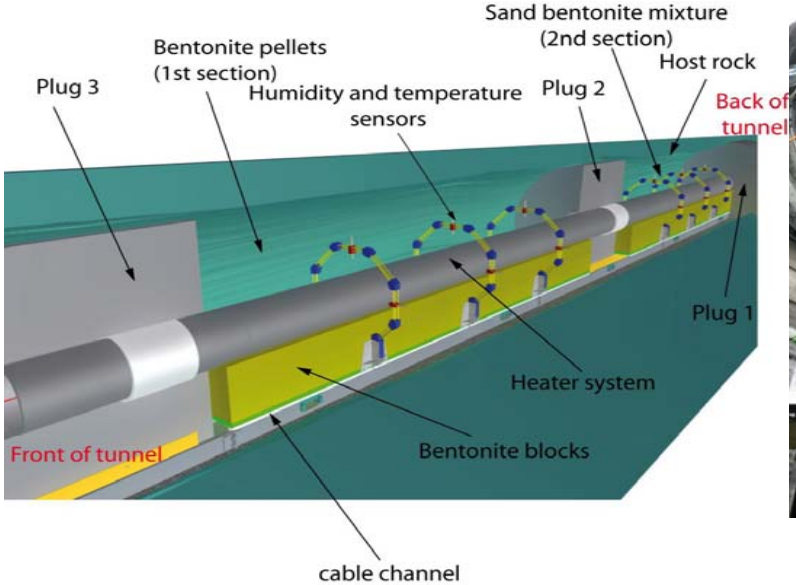

Mont Terri FE Test Modeling

INITIAL 2D TOUGH-FLAC ANALYSIS:

- *Inclined TOUGH2 mesh for capturing TH anisotropy in rock*
- *Ubiquitous joint model for capturing anisotropic strength properties in rock*
- *Barcelona Basic Model for bentonite (pellets and blocks)*

Alt. 1

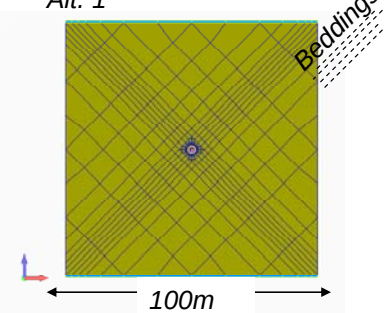

Alt. 2

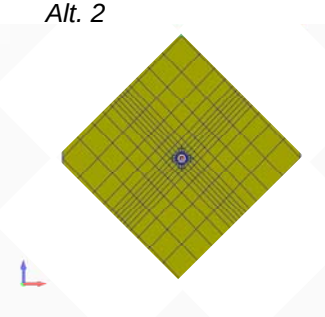

Far field TOUGH mesh aligned with 45 degree beddings (need anisotropic thermal and hydraulic properties)

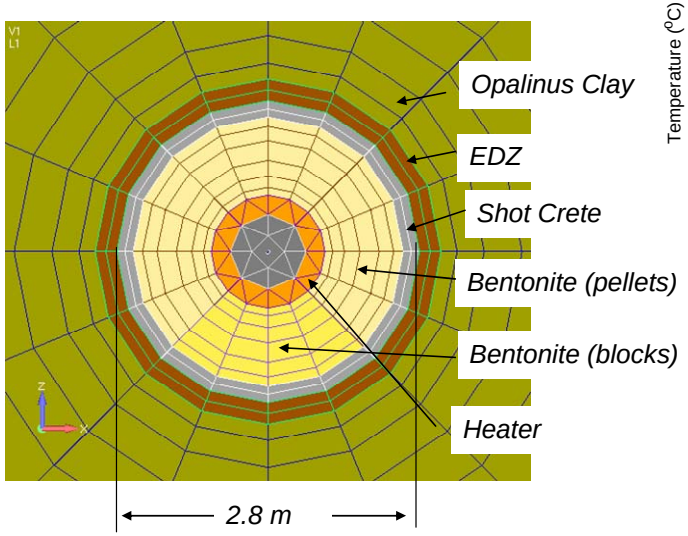

Preliminary results (IHLRW 2013)

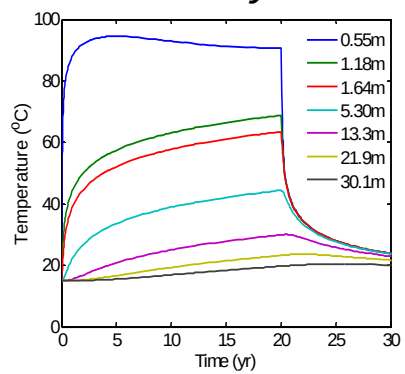

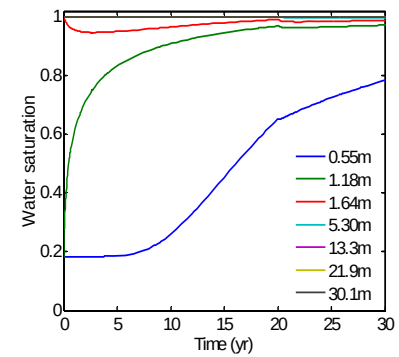

Next steps:

Extend to full 3D

Determination of THM parameters for bentonite pellets

Thermal Limit Testing: LBNL High Temperature Laboratory Experiments

Objective

Investigate the impact of heat-induced chemical alterations (smectite-to-illite transformation) of buffer and backfill materials (bentonite) and clay host rock on their geomechanical and hydrological properties (mechanical strength, permeability, seismic velocity)

Approach

- **Test bentonite and opalinus clay (in-situ samples) with a range of (1) porosity (density), (2) water content (below saturation), (3) KCl concentration**
- **Multiple samples are heated (from 100° C to 300° C) in sealed, spring-loaded cylindrical miniature pressure vessels**
- **Chemically inert material (Titanium, will be passivated) is used for the equipment**
- **Changes in volume, acoustic velocity, permeability, and mechanical strength are examined for different heating durations**
- **Chemical/mineral testing in collaboration with LANL**
- **Integration with modeling work (TOUGHREACT-FLAC3D)**

Miniature pressure vessel
(“test tube”)

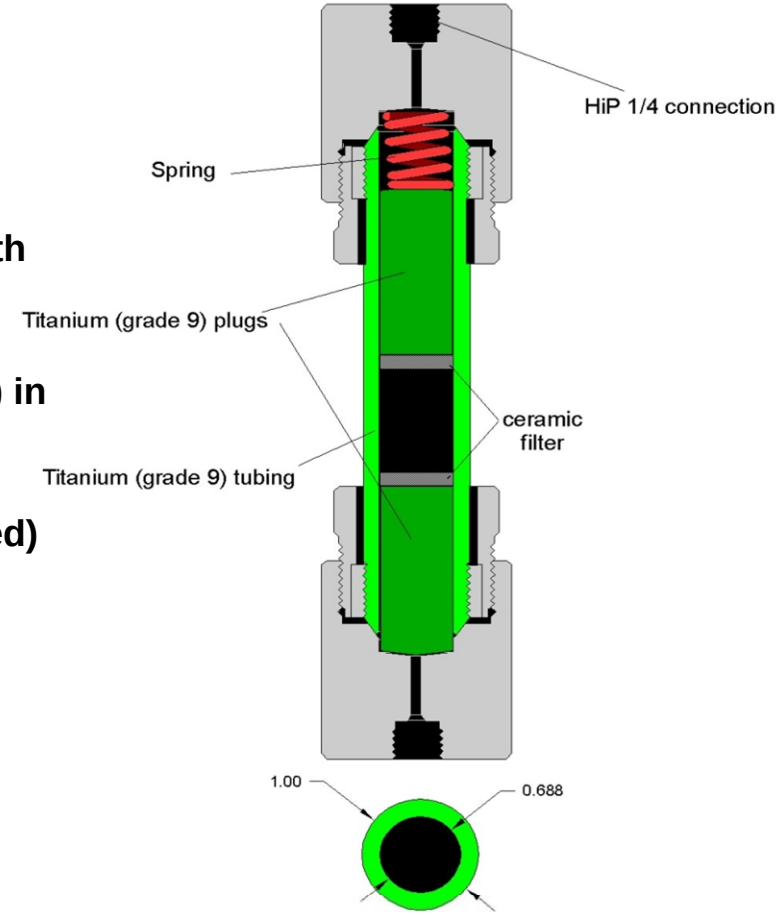

Thermal Limit Testing: LBNL High Temperature Laboratory Experiments

Current Status

- **Commercial, Ti-5 pressure vessel fabrication (scheduled completion Jan.18)**

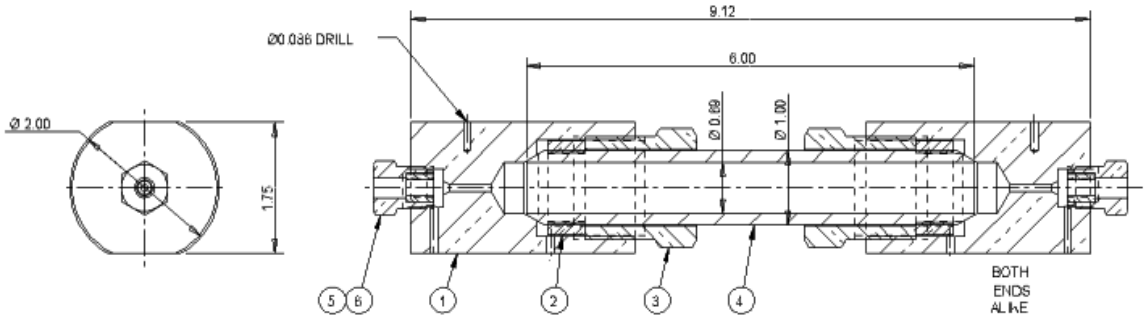

- **Collaboration with NAGRA—Mont Terri cores will be used for our experiments: (i) Stock core will be shipped to LBNL in Jan 2013; (ii) New drilling campaign for fresh cores in May 2013**

NAGRA—Mont Terri cores

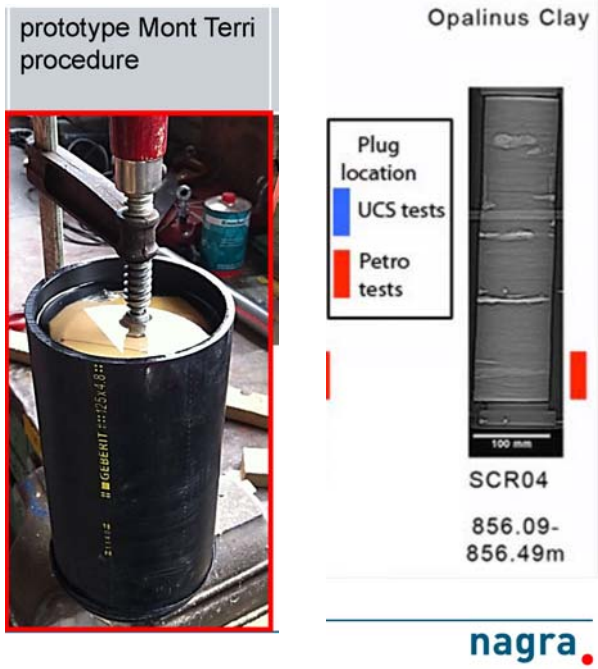

Image courtesy: Dr. Müller Herwig (Nagra)

Thermal Limit Testing:

Detailed Mechanistic Modeling of THMC Alterations

Investigation of the Maximum Allowable Temperature in a Clay Repository using detailed mechanistic models

Motivation:

- ❑ Illitization which results in a loss of swelling capability of EBS and clay host rock, could be enhanced as temperature increases.
- ❑However, many factors such as the availability of potassium, proton and water constrain the illitization. A model that could consider all the relevant factors is needed to evaluate the illitization in EBS and clay host rock.
- ❑The mechanical and hydraulic consequences of illitization also need to be evaluated.

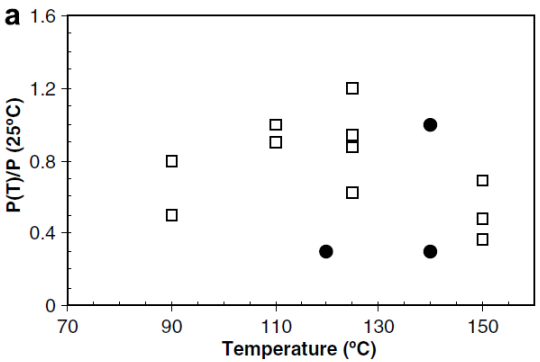

Swelling pressure

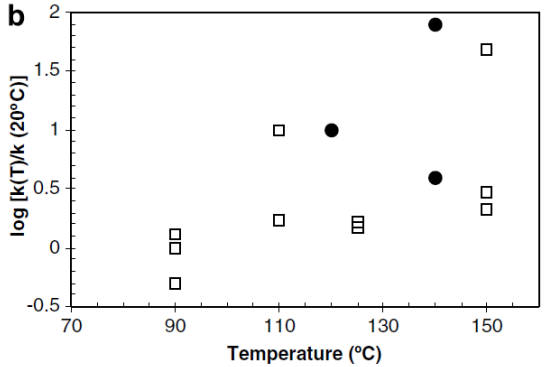

Hydraulic conductivity

Thermal Limit Testing:

Detailed Mechanistic Modeling of THMC Alterations

Will illitization ***in EBS*** be enhanced if more heat is released from canister (higher temperature)?

1-D model:

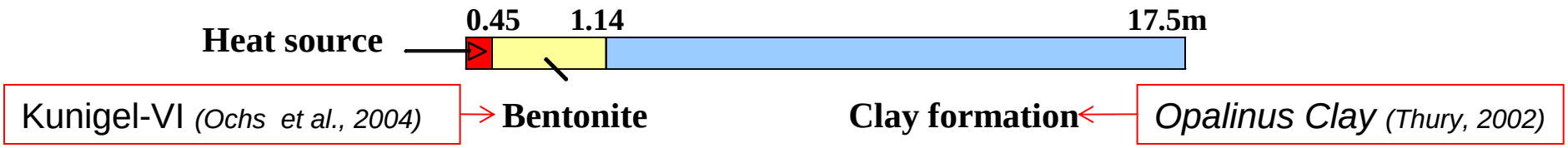

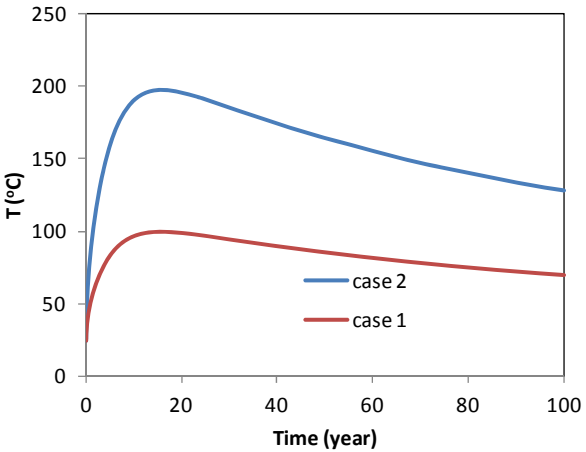

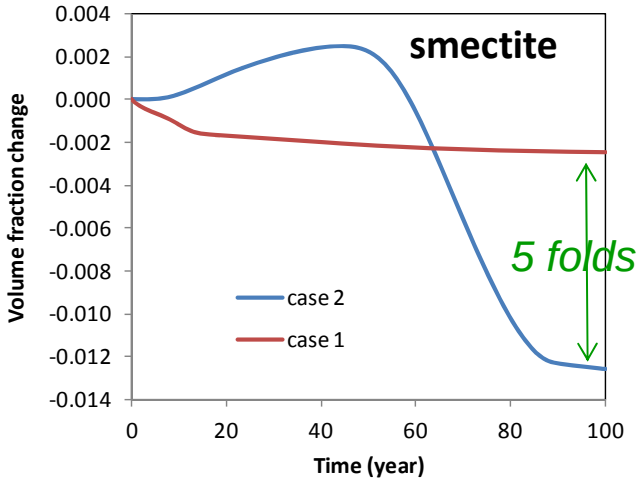

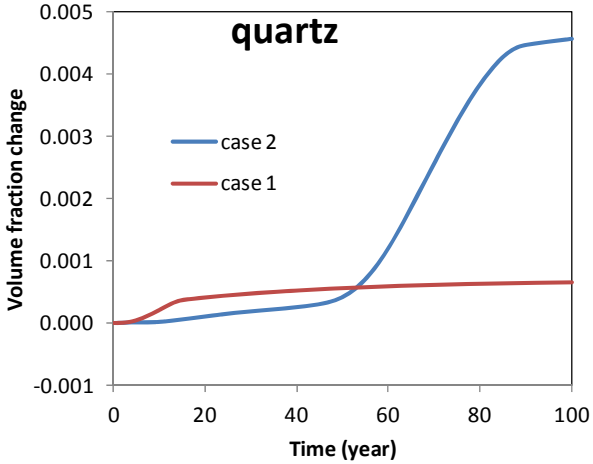

Time evolution of T, smectite, quartz at a point near the canister ; More smectite is losing; Precipitation of quartz raises the issue of cementation of EBS;

Used Fuel Disposition Campaign

Coupled THM discrete model for argillaceous rock

Daisuke Asahina, Jim Houseworth, and Jens Birkholzer

Lawrence Berkeley National Laboratory

UFD NBS Telecom

January 08, 2013

Presentation outline

- Introduction
- Discrete fracture network
- Mechanical damage model
- Coupling THM model with fracture
- Summary and research directions

Used Fuel Disposition

Coupled thermal-hydrological-mechanical (THM) discrete fracture model (DFM) for argillaceous rock

- **Argillaceous formations that may be available for nuclear waste disposal are typically saturated**
  - Suitability of argillaceous rock rests in large part , on an effective and robust low-permeability attribute
- **Fracturing is the most likely threat to the low-permeability attribute of an argillaceous rock:**
  - Repository-induced THMC disturbances cause fracturing along repository openings
  - Natural disturbances (e.g., abnormal pressure – induced hydrofractures) cause fracturing at the formation scale
- **Fractures in argillaceous rock tend to be short-lived because of self-sealing behavior**
  - Can lead to poorly-connected fractures during fracturing episode
  - Potential fracture-matrix cross-flow interaction
  - Coupled process DFMs more representative

Blümling et al., 2007

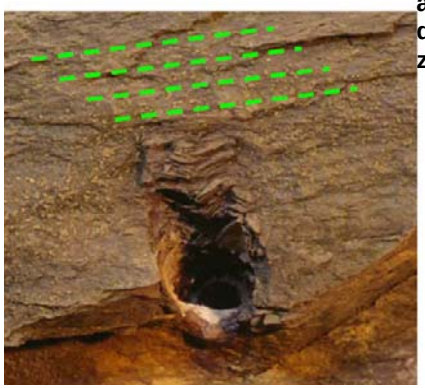

flow focusing along damage zone

Modified from Bauer et al., 2003

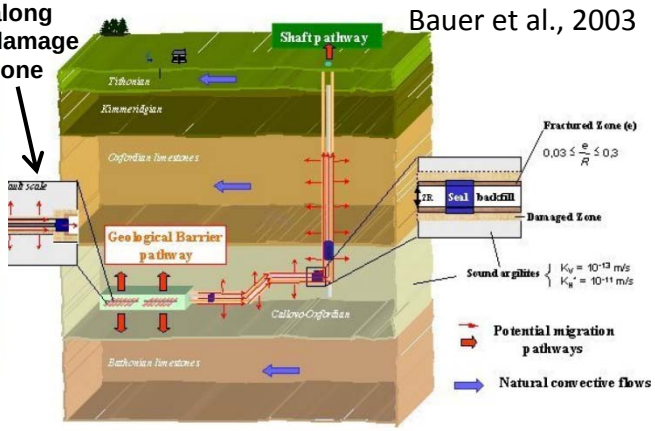

Mercia Mudstone, Bristol Channel Basin, UK: natural hydraulic fractures filled with sand and gypsum

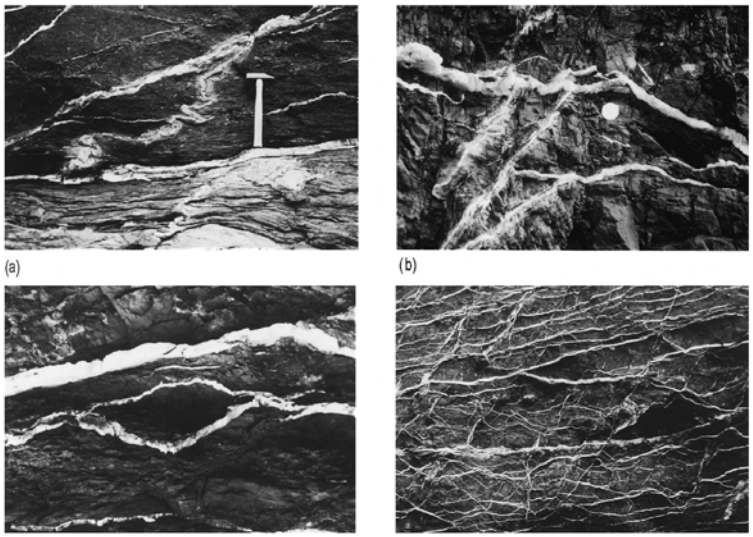

Cosgrove, 2001

Discrete Fracture Network(DFN): issues

- **Flow and Transport**
  - initially dense fracturing that can evolve into sparse set of irregular open fractures with complex interconnections over a relatively small domain
- **Geomechanics**
  - Fractures form or reactivate in response to a perturbation and evolve, generally resulting in self-sealing/healing of fractures
- **Significant issues for discrete fracture models are**
  - complex fracture geometry
  - evolving fracture network

Direct Mapping Approach for discrete fracture

Step:

1. *Generate Voronoi grid*
2. *Map fracture configuration onto the grid*
3. *Use edges of Voronoi cell to represent discrete fracture*

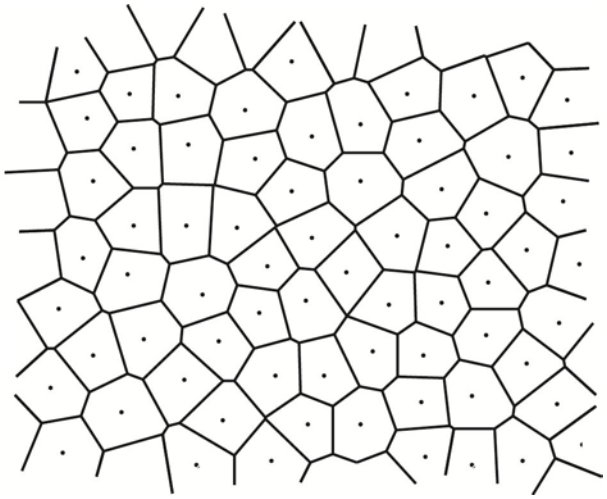

- Advantages include
  - Relatively simple activation and connection of new fracture
  - Fracture intersections automatically included; no degenerate fracture network geometry
  - Straightforward extension to 3D

- Disadvantages include
  - Less control of fracture geometry
  - Uses more nodes

Application Example for DRZ

Bossart et al., 2004

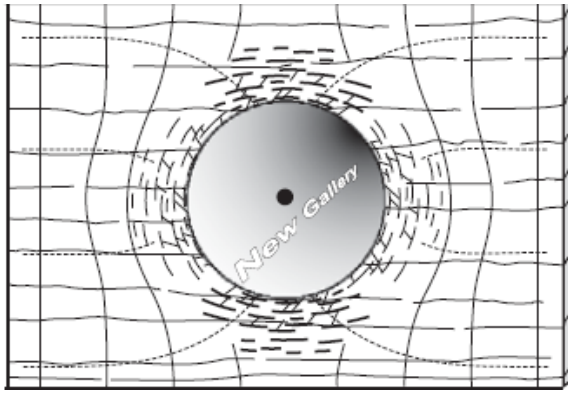

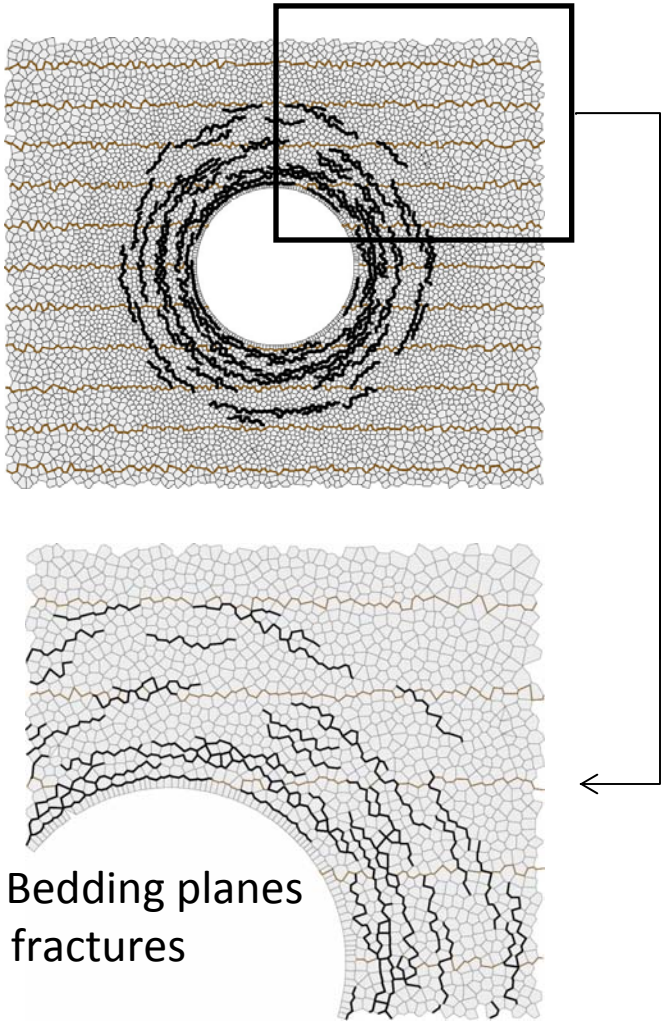

- fracture nodes and connections

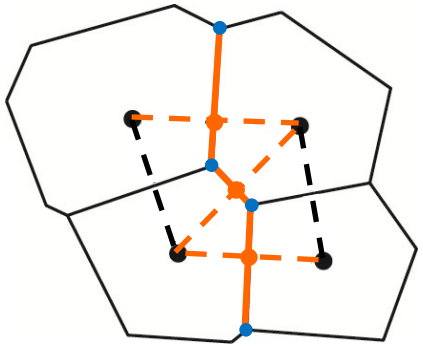

- Bedding planes & fractures

Mapping of a fracture geometry on top of an irregular Voronoi grid.

Hydrogeologic modeling of discrete fractures

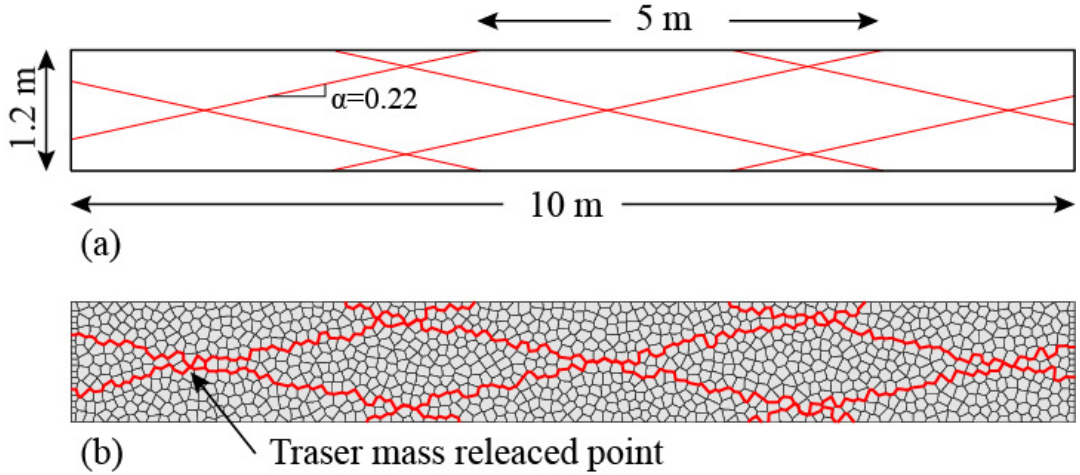

DFNs in Voronoi grid (1097 matrix nodes and 503 fracture nodes)

Simulation parameters

• Fracture permeability (m^2)	3.7×10^{-13}
• Matrix permeability (m^2)	1.0×10^{-18}
• Fracture aperture (m)	0.001
• Fracture porosity	0.087
• Matrix porosity	0.2
• Diffusion coefficient(m^2/s)	1.0×10^{-11}

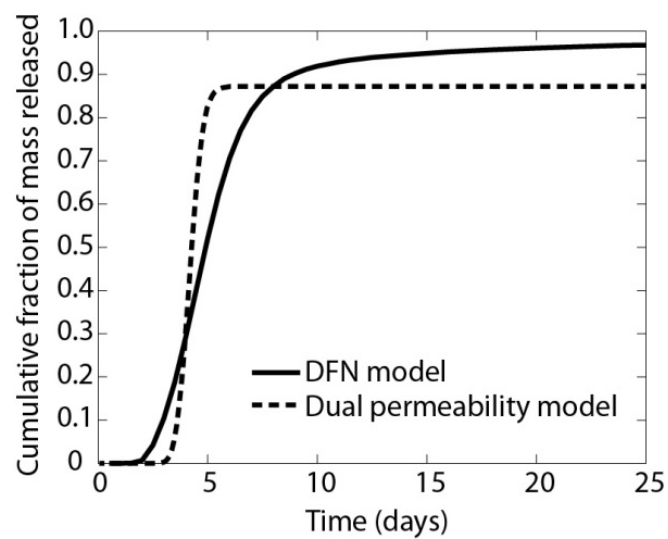

Mechanical Damage Models: Rigid-Body-Spring Network (RBSN)

Rigid-body-spring network

- Element network is Delaunay/Voronoi
- Mechanical spring set is located at the centroid of Voronoi cell boundary
- Small-deformation method
- Program code is written in FORTRAN77

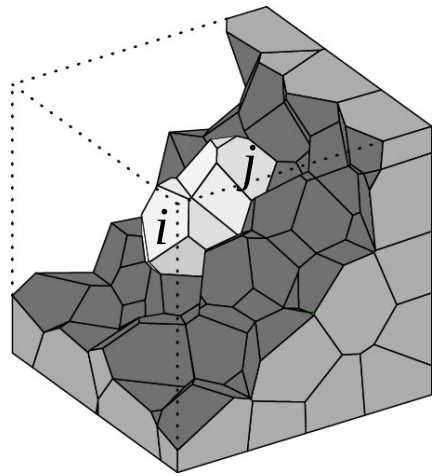

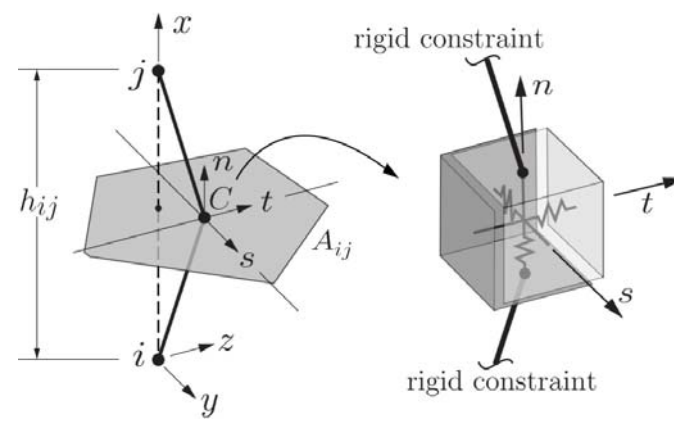

element unit ij

Local stiffness terms

$$k_x = k_y = k_z = E\frac{A_{ij}}{h_{ij}}$$

$$k_{\phi x} = E\frac{J_p}{h_{ij}}\ ,\ \ k_{\phi y} = E\frac{I_{tt}}{h_{ij}}\ ,\ \ k_{\phi z} = E\frac{I_{ss}}{h_{ij}}$$

References for RBSN:
- Kawai, 1978
- Bolander and Saito, 1998
- Asahina et al., 2011

Fracture representation

- *Mohr-Coulomb surface*

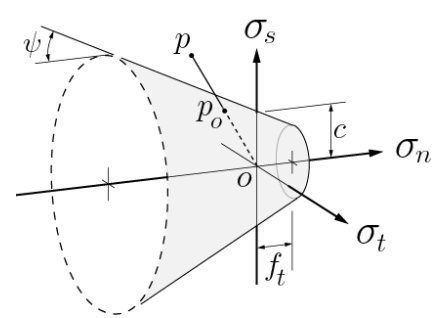

- *Vectorial stress approach*

$$\sigma_R = \frac{F_R}{A_{ij}^p}$$

F_R : *resultant force*

A_{ij}^P : *projection area perpendicular to* F_R

Rigid-Body-Spring Network (RBSN): Motion of basic element unit

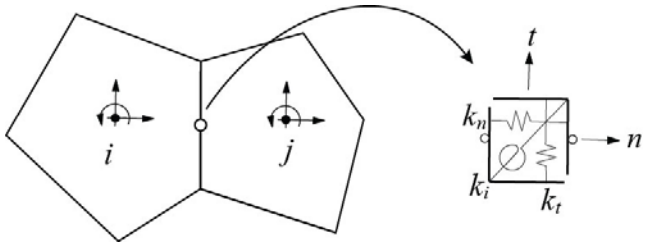

spring set

normal direction 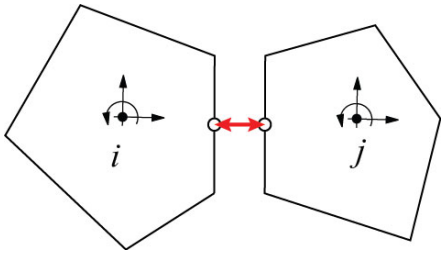	**rotation** 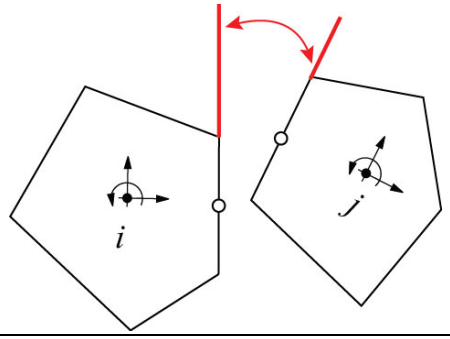
tangential direction 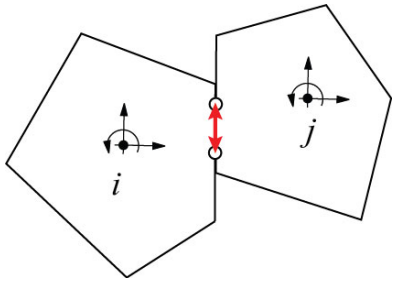	**overlapping** 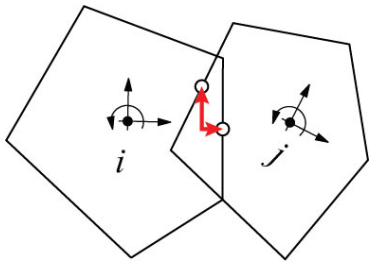

Rigid-Body-Spring Network (RBSN): Numerical examples

3-point bend test
(Bolander et al., 2003)

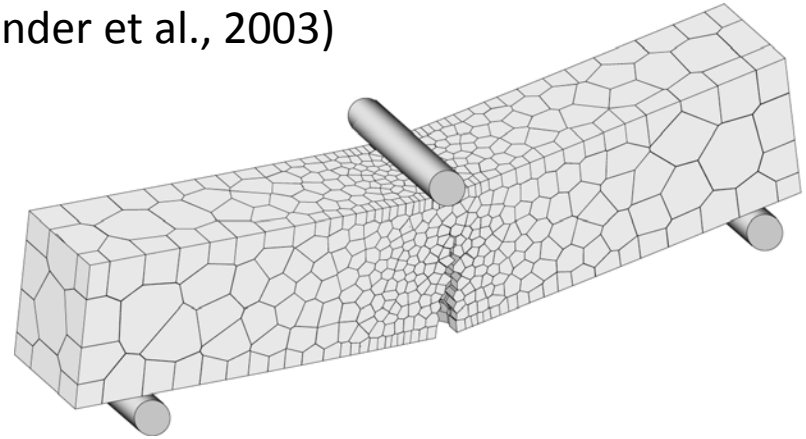

Uniaxial compression

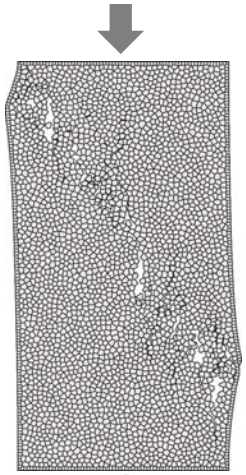

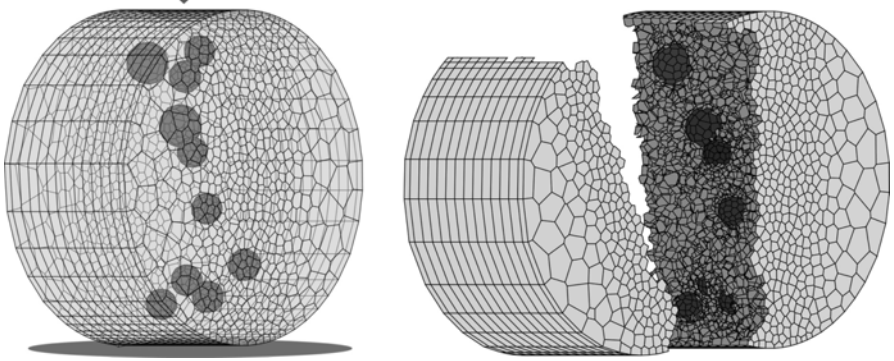

Split cylinder test (Asahina et al., 2011)

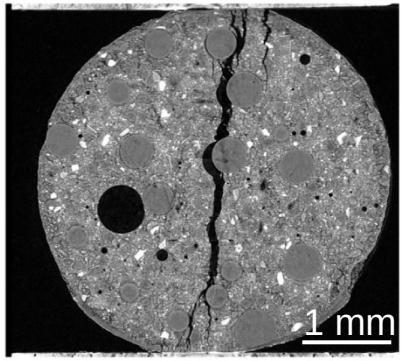

Micro-CT image

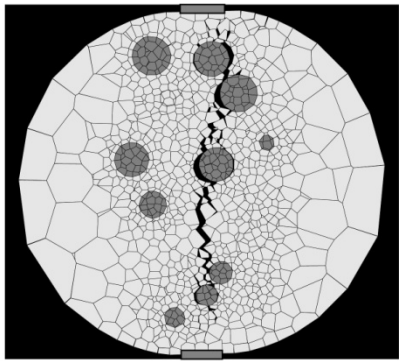

Simulation results

Coupling thermal-hydrologic flow and geomechanics

Program	TOUGH2	RBSN
Physics	Thermal-hydrologic Flow	Geomechanics (elasticity, fracture)
Primary Values	Temp, Pressure, Saturation	Displacement, force
Method	FVM	Discrete model
Grid	Voronoi	Voronoi

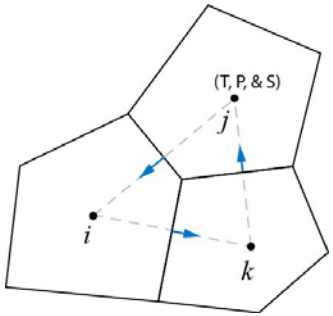

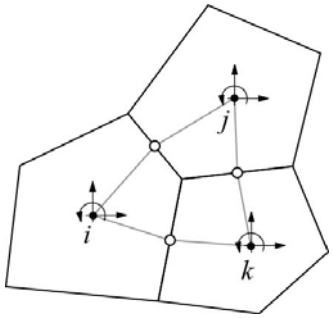

- Two models share same grid information

TOUGH-RBSN verification 1: swelling pressure tests

- Fully confined
- Wetted to full saturation

Dry density : 1.6 g/cm^3
Initial saturation : 65%
Swelling coefficient : 0.238
Bulk modulus : 20 MPa

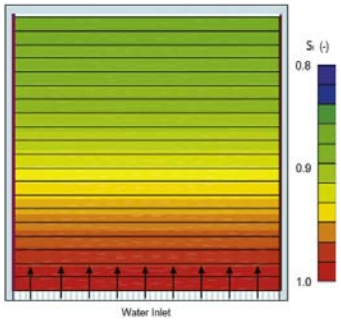

(Rutqvist, 2010)

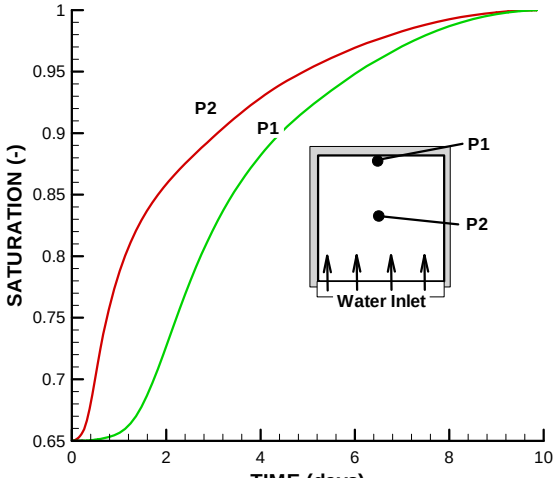

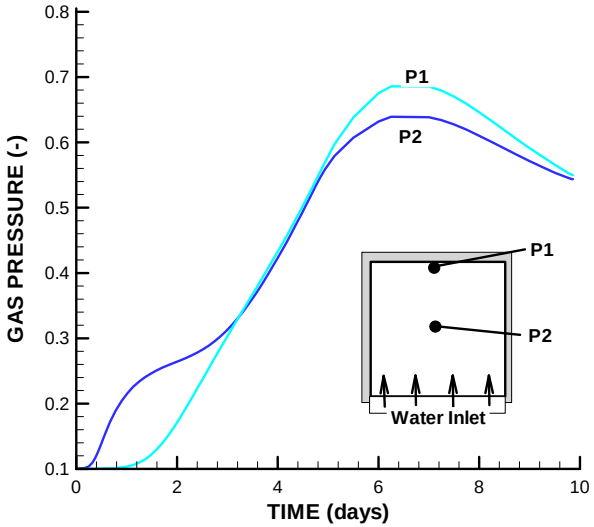

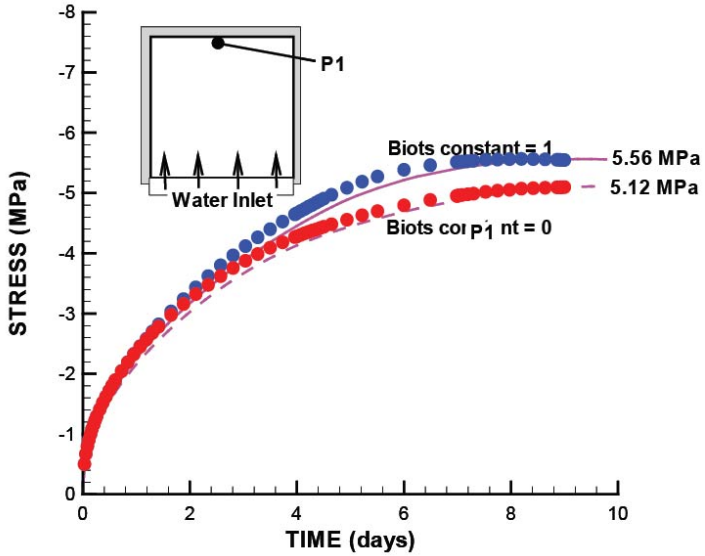

TOUGH-RBSN verification 2: thermalstress analysis

- Domain: 2mx2m
- Radius of borehole: 0.075m
- Elastic modulus : 50 Gpa
- Poisson Ratio : 0.17
- Thermal conductivity coefficient : 1.0 $W \cdot m^{-1} \cdot K^{-1}$
- Volumetric thermal expansion coefficient : 1×10^{-6} $^{\circ}C^{-1}$

(by Lianchong Li, et al. 2012)

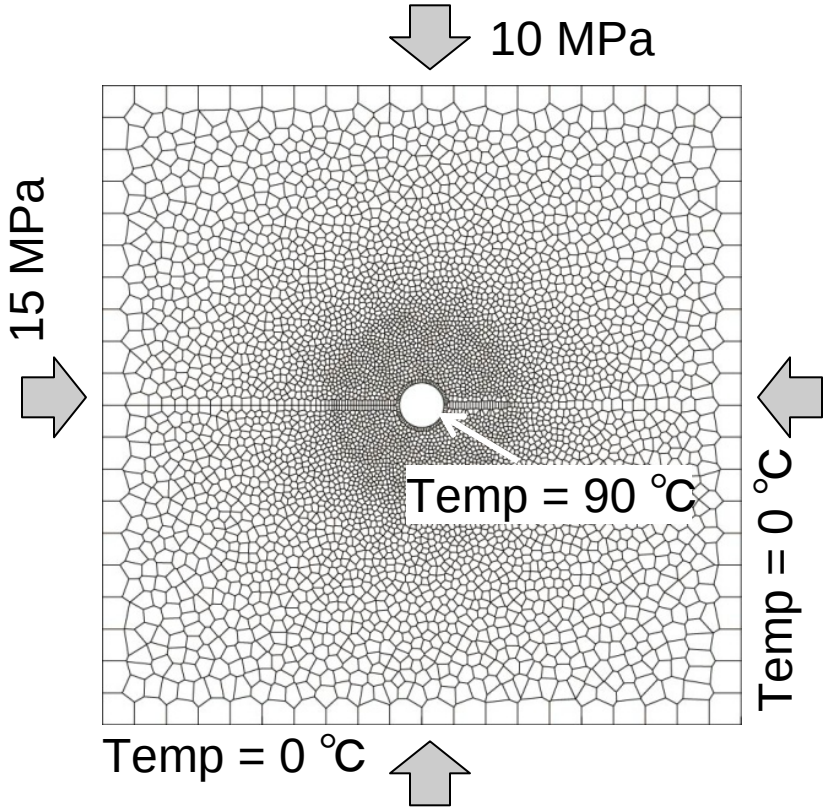

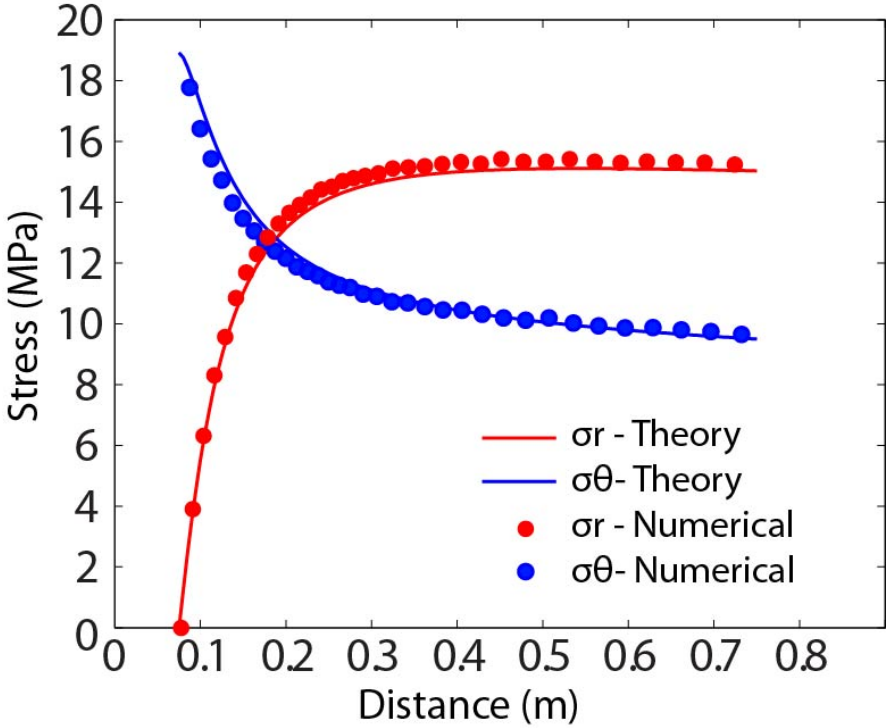

TOUGH-RBSN simulation: desiccation shrinkage cracking

Experimental observation (Rodriguez et al. 2007):
distance between cracks increases with material thickness

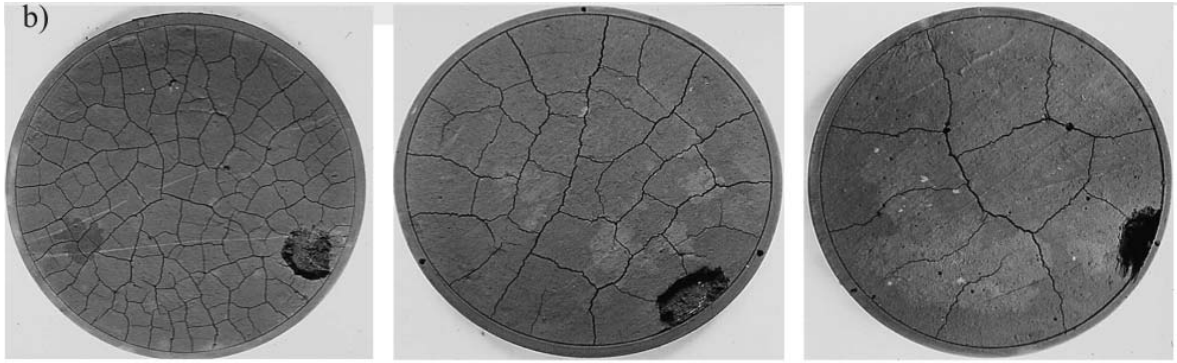

Thickness = 4 mm 8 mm 16 mm

TOUGH-RBSN simulation in 2D

4mm

8mm

16mm

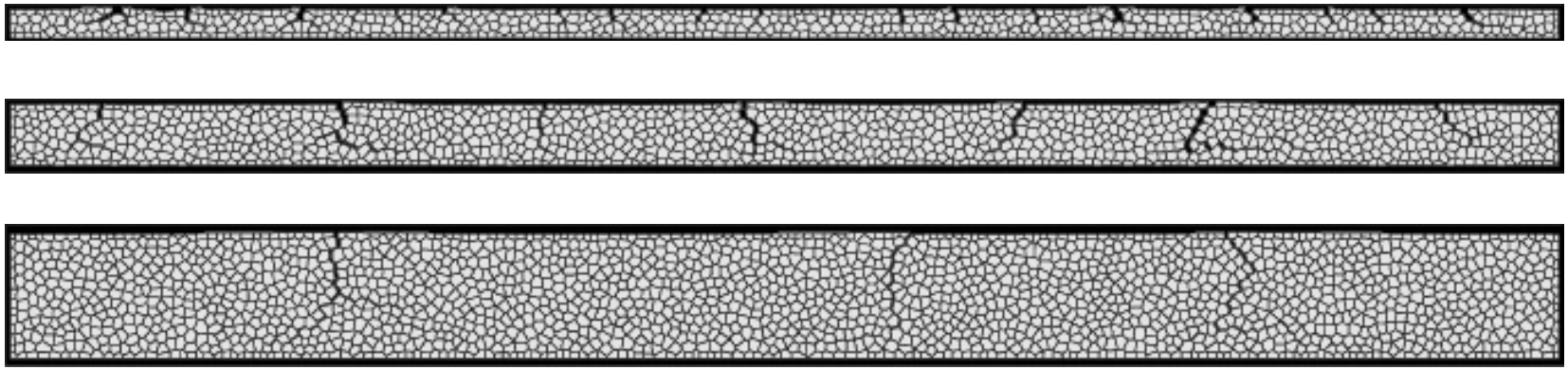

TOUGH-RBSN simulation: desiccation shrinkage cracking

Experimental results
(thickness = 8mm)

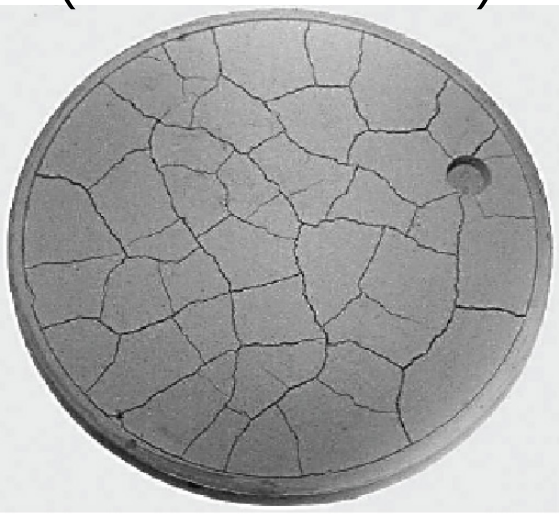

Diameter of specimen: 225 mm

TOUGH-RBSN
simulation results

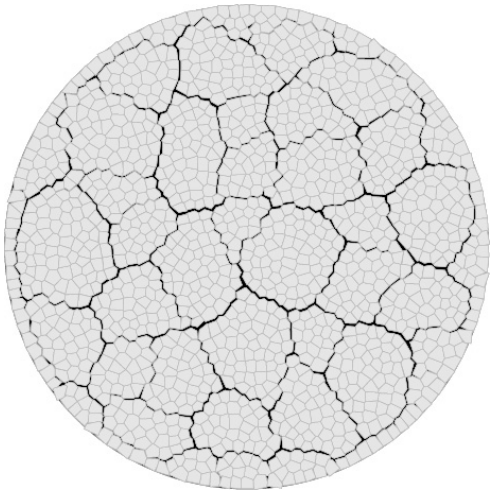

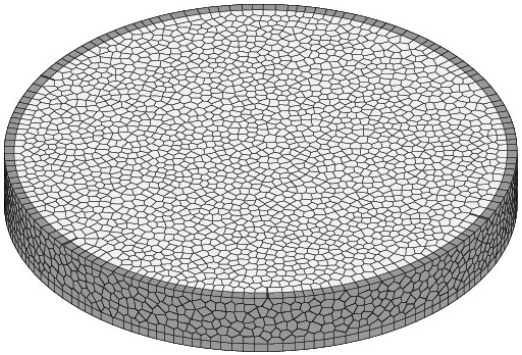

3-D simulation

TOUGH-RBSN simulation: Flow through fractures (ongoing research)

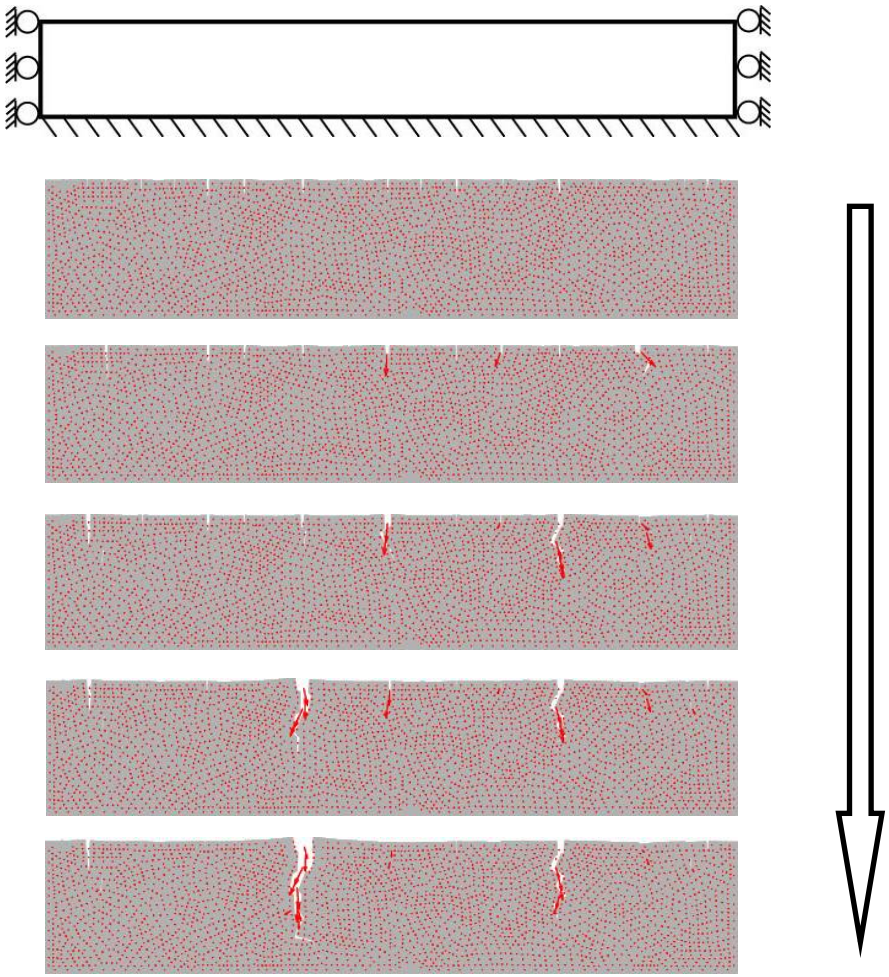

- fracture nodes and connections

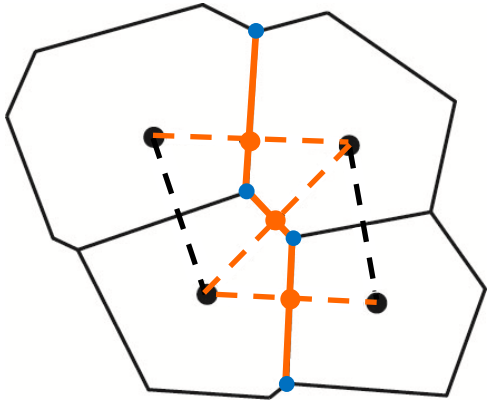

- Fractured regions are more permeable than the intact matrix

Summary

- A 3D THM model with fracture propagation has been developed.
- The model adds the capability to simulate a dynamic process of flow-fracture interaction.

Research directions

- Investigating fracture propagation induced by excavation as well as fluid overpressure
- Investigating the ventilation process of EDZ (swelling/desiccation)
- Simulating self-sealing process of fractures

Used Fuel Disposition Campaign

Constitutive Relationships for Clay Rock

Hui-Hai Liu, Lianchong Li and Jens Birkholzer
(LBNL)

Jan 8, 2013

Constitutive Relationships

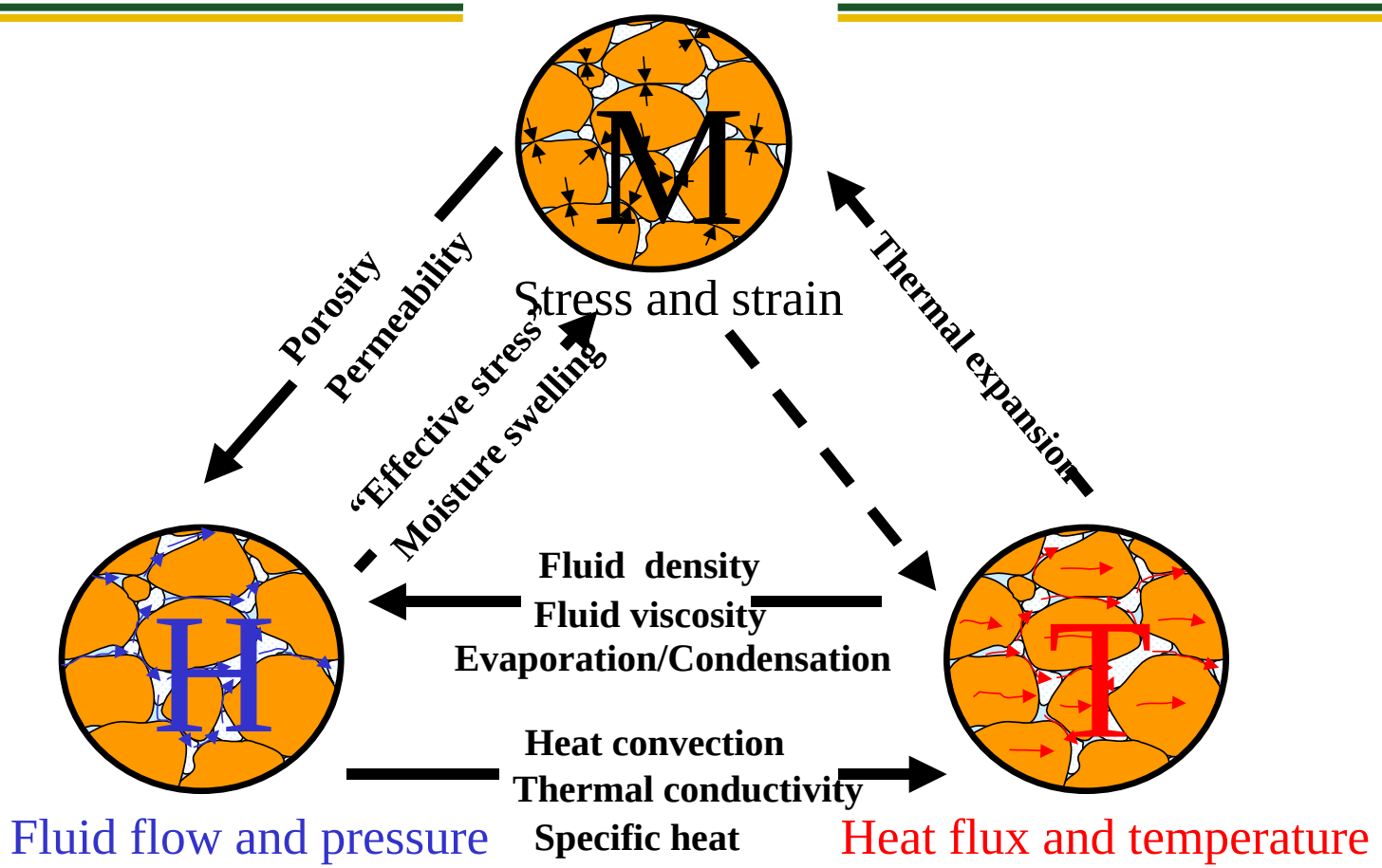

The constitutive relationships refer to relationships among hydrological, mechanical, and other properties. They define how coupled processes are coupled in a numerical model.

Constitutive Relationships:
Challenges and Research Focus

Challenges:

- Clay mechanical behavior is strongly moisture dependent
- Fracture properties are important for processes in EDZ, but approaches to calculate them are not well established when swelling/shrinkage is involved.
- Traditional fluid-flow theories need to be revisited because of nano-scale pore sizes

Current Research:

- Two-part Hooke's model (TPHM) for modeling mechanical deformation and stress-dependent hydraulic properties.
- Non-Darcian water flow.

Two-Part Hooke's Model (TPHM)

- **Hooke's Law**:

$$d\sigma = K d\varepsilon_v$$

- **Engineering and true (natural) strains**

$$d\varepsilon_{v,e} = -\frac{dV}{V_0} \qquad d\varepsilon_{v,t} = -\frac{dV}{V}$$

- **"Two-Parts" model:**

A rock body can be divided into two parts: the hard part and soft part (that corresponds to a fraction of pore volume subject to a large degree of relative deformation [such as cracks])

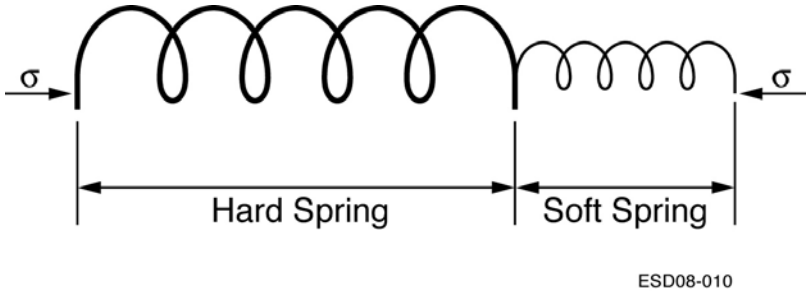

•Stress-Strain Relationship (Liu et al. 2009)

$$-\frac{dV}{V_0} = \gamma_e \frac{d\sigma}{K_e} + \gamma_t \frac{d\sigma}{K_t} \exp\left(-\frac{\sigma}{K_t}\right)$$

$$\gamma_t = \frac{V_{0,t}}{V_0} \qquad \gamma_e = 1 - \gamma_t$$

TPHM: Comparison with lab data

$$-\frac{dV}{V_0} = \gamma_e \frac{d\sigma}{K_e} + \gamma_t \frac{d\sigma}{K_t} \exp\left(-\frac{\sigma}{K_t}\right)$$

Data are for Oplinus clay rock (Cokum and Martin, 2007)

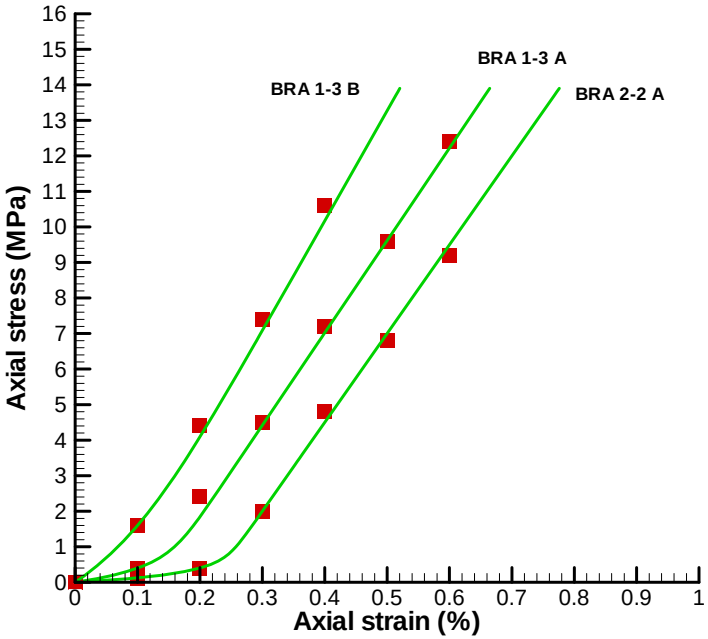

Rock Sample	γ_t (%)	K_e (MPa)	K_t (MPa)
BRA 2-2A	0.22	2494.5	0.22
BRA 1-3A	0.13	2596.6	0.38
BRA 1-3B	0.08	3097.6	0.65

TPHM: Modeling Fracture Permeability Evolution for a clay sample

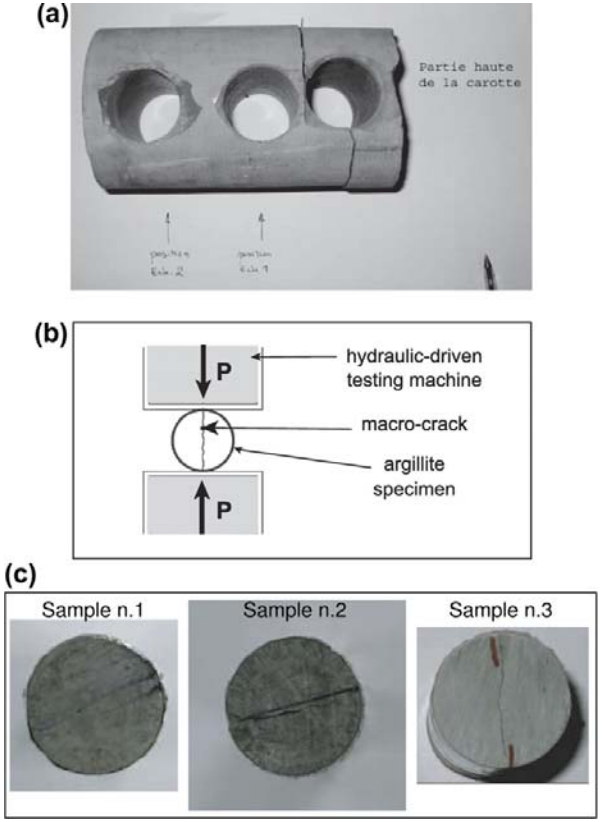

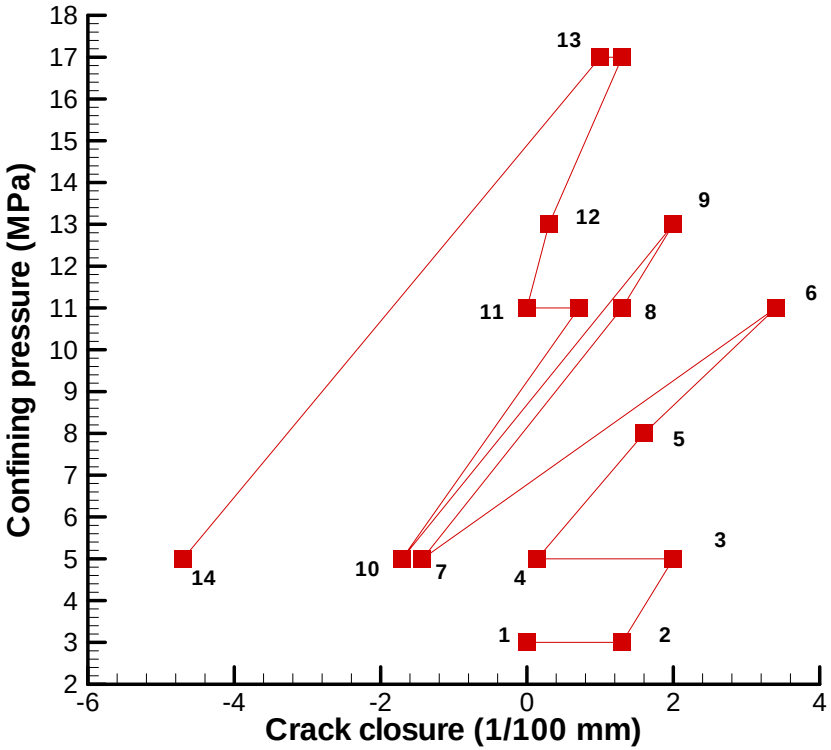

Test procedure of water permeability measurement (in terms of confining pressure and fracture [crack] closure) for sample 2 of Davy et al. (2007). The numbers in the figure indicate the chronological order of points .

TPHM: Internal Swelling Stress

- **Internal swelling stress**

$$\sigma = \sigma_t - \alpha P + \sigma_I$$

- **Clay-matrix strain resulting from swelling**

$$\varepsilon_s = \varepsilon_{sB} + \varepsilon_{sI}$$

- **Assumption**

$$\varepsilon_{sI} \approx f\varepsilon_s$$

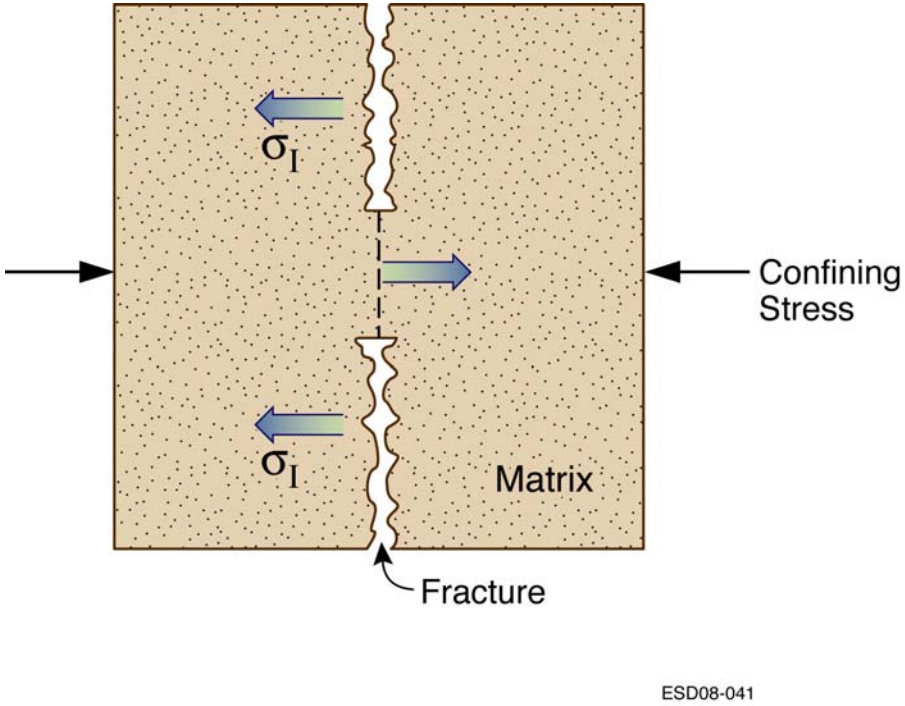

TPHM: Analysis of Experiment Results

- **Generalized effective stress**

$$\sigma = \sigma_t - \alpha P + \sigma_I$$

- **Permeability**

$$\left(\frac{k}{k_3}\right)^{1/3} = \exp\left(-\frac{\Delta\sigma_t}{K_{F,t}} - Bt^{1/2}\right)$$

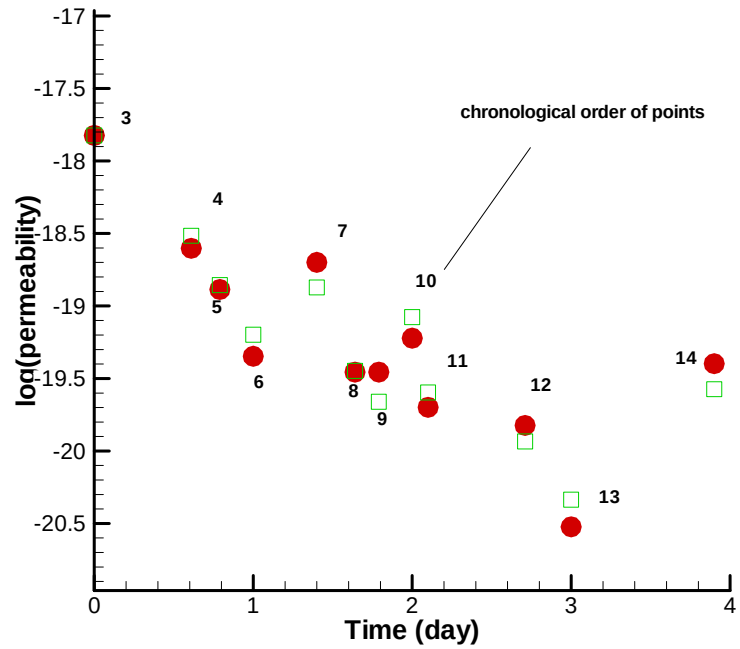

Comparisons between observed and simulated fracture permeability changes as a function of time. The solid circles are measurements

TPHM: Simulation of Displacement Field

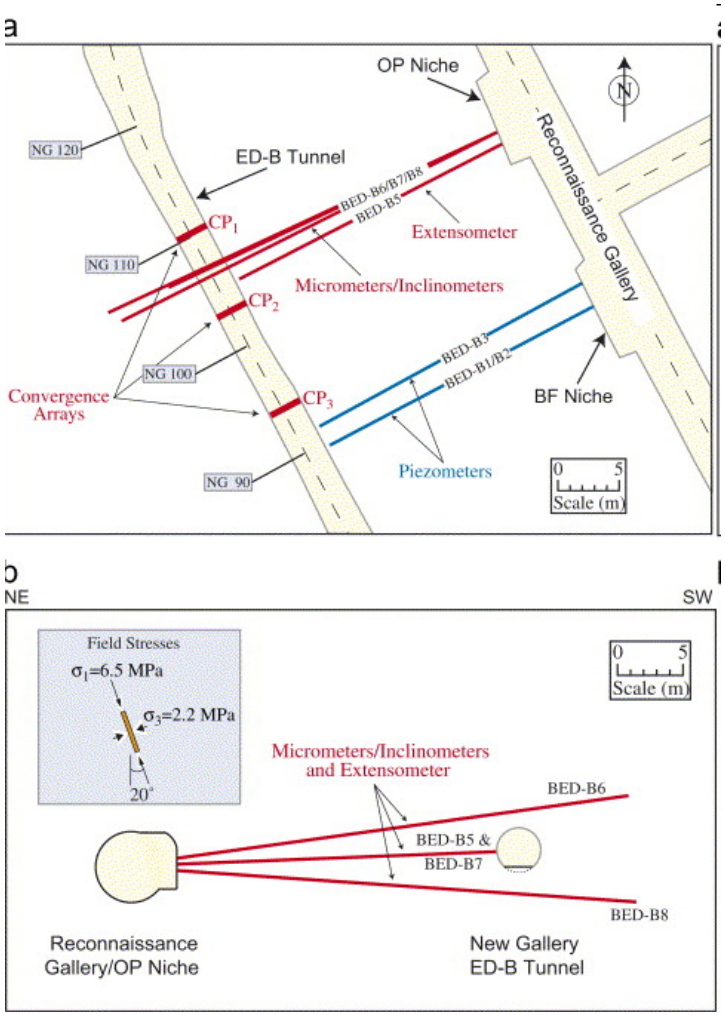

A mine-by test at the Mont Terri Site

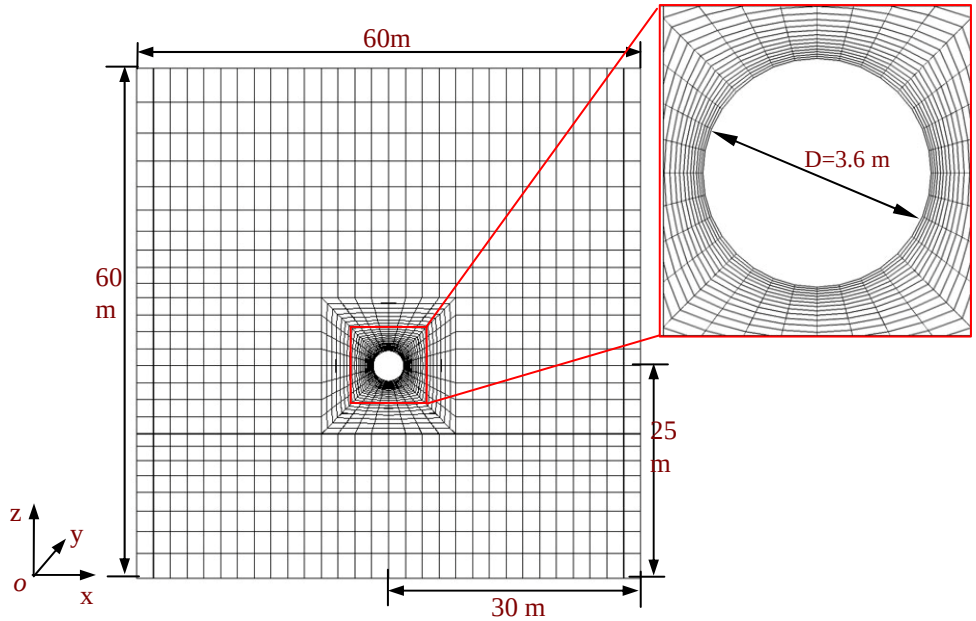

TPHM: TOUGH-FLAC Simulation Results

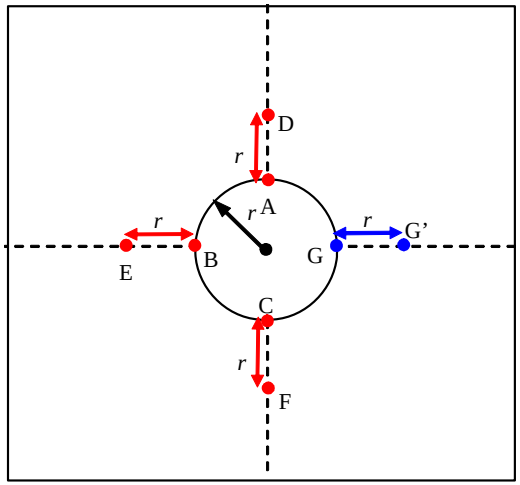

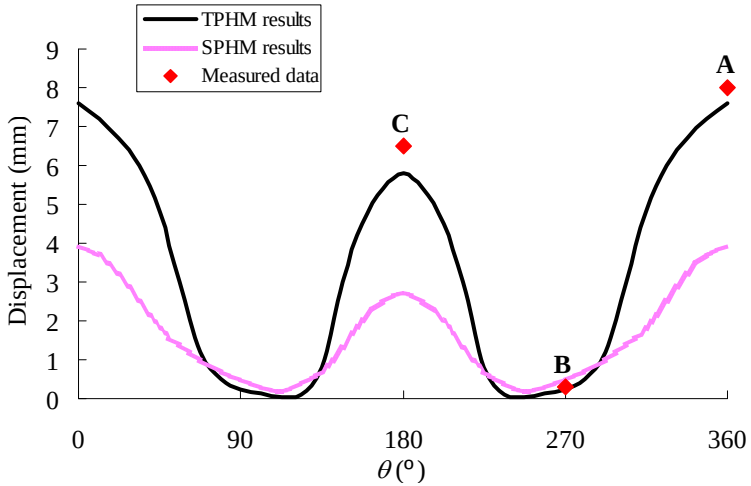

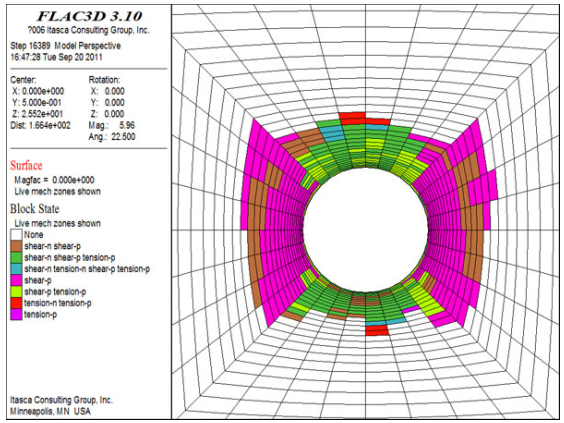

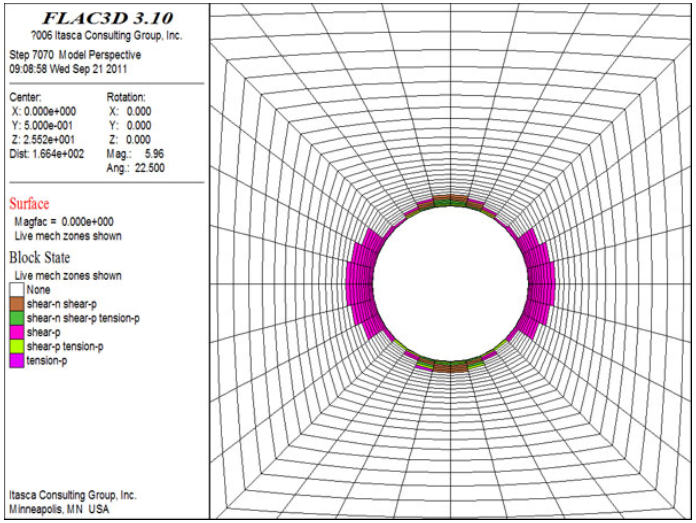

Darcian and Non-Darcian Flow

- Henry Darcy (1856) discovered Darcy law that water flux is proportional to hydraulic gradient.
- In some cases, Darcy law does not hold.
- Considerable effort has been made in modeling non-Darcian flow for high Re values (or high flux) [Forchheimer (1901) Law]
- Our interest here is water flow behavior in [low-permeability] clay.

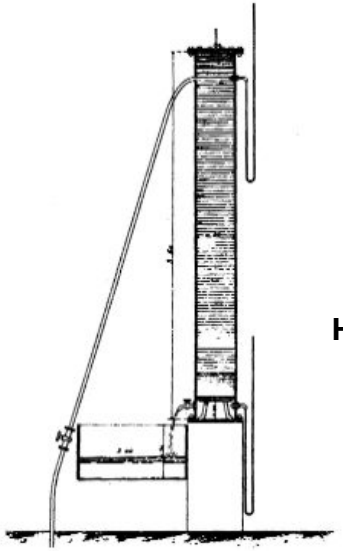

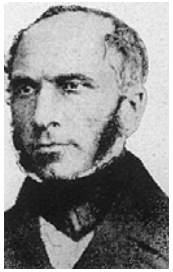

Henry Darcy

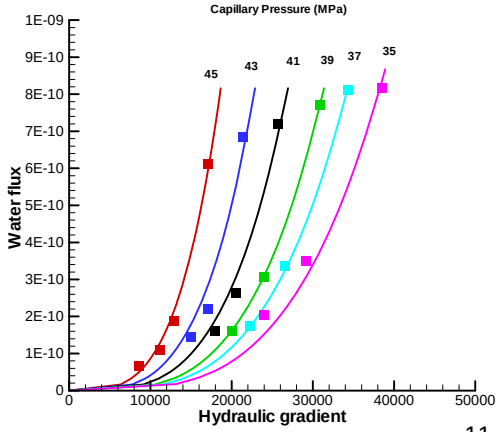

Importance of Non-Darcian Flow

- Excavation Damaged Zone (EDZ) is a critical feature impacting repository performance.
- Desaturation and resaturation are important for EDZ evolution (shrinkage-induced fracture; fracture self-sealing).
- Water flow from host rock to EBS is critical for buffer to function (swelling).

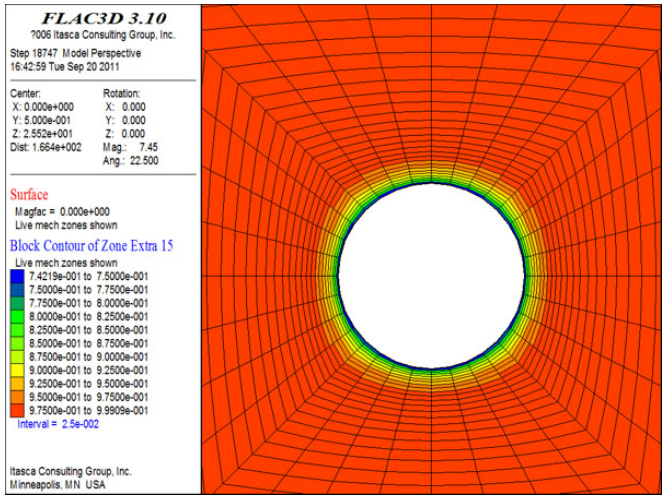

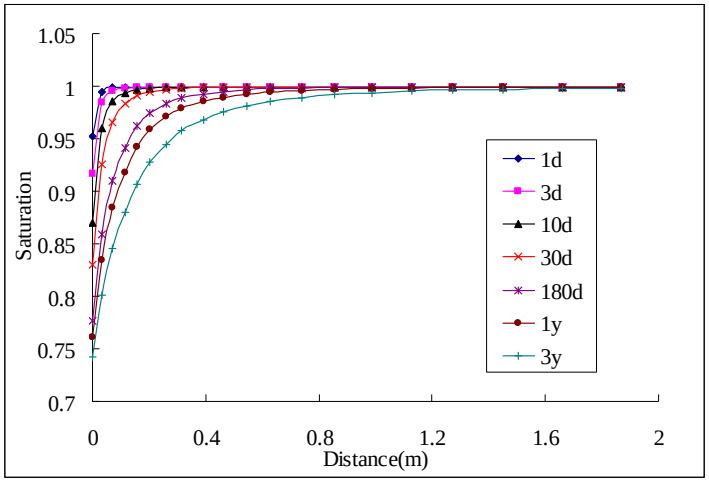

Evidence: Laboratory Experiments

- A relative comprehensive literature survey has been performed.
- Test data sets show the existence of non-Darcian flow behavior for clay media.
- Unsaturated flow corresponds to a large degree of non-Darcian flow.
- The behavior may be a result of strong water-solid interaction (Low, 1961).

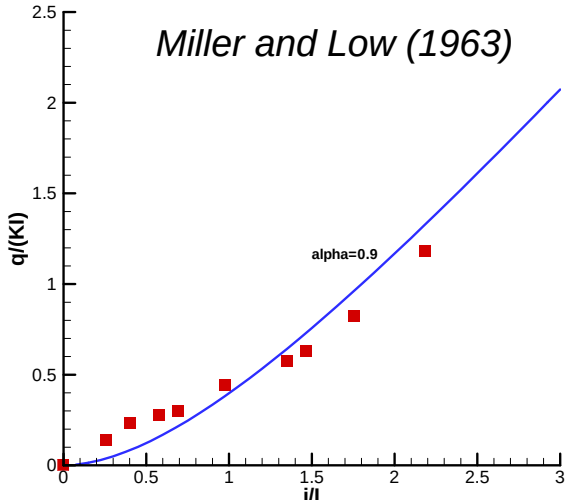

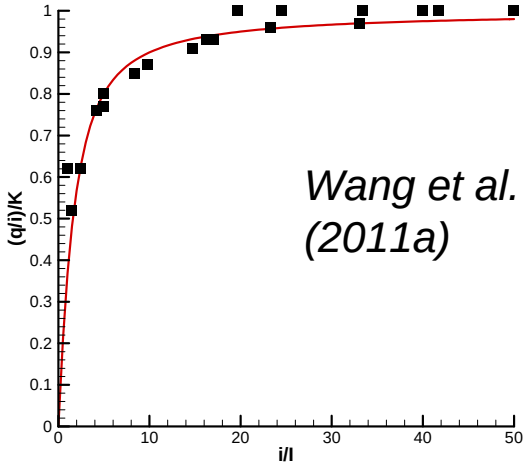

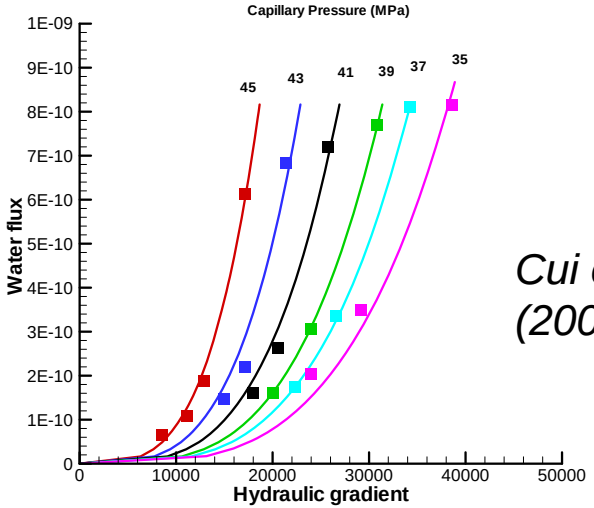

Evidence: Nanoscale Flow Simulation

Chen et al. (2008)

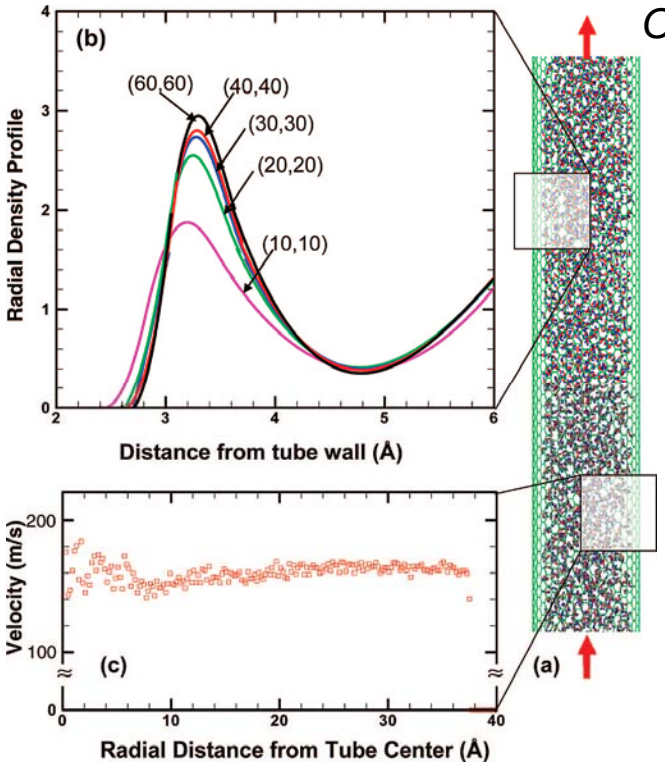

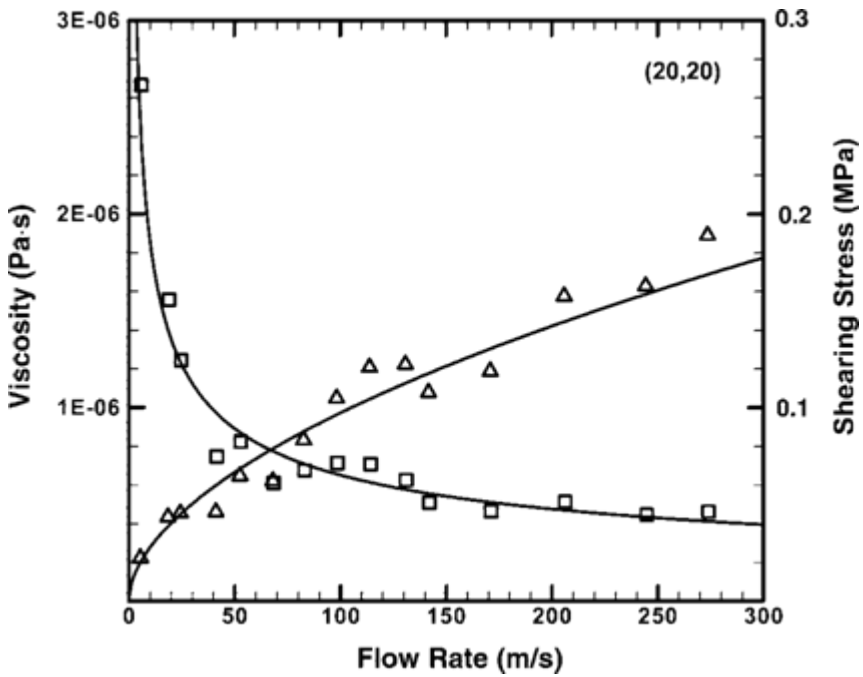

- *Nanoscale water properties are very different from those for bulk water (Wang et al., 2011b)*
- *Molecular dynamic simulation results support the existence of non-Darcian flow in clay.*

Relationship between water flux and hydraulic gradient

Threshold gradient model

$$q = K(i - I)$$

Swartzendruber (1961):

$$q = K[i - I(1 - e^{-i/I})]$$

Proposed model:

$$q = K[i - \frac{I}{\gamma(\frac{1}{\alpha})}\gamma(\frac{1}{\alpha}, \left(\frac{i}{I*}\right)^{\alpha})]$$

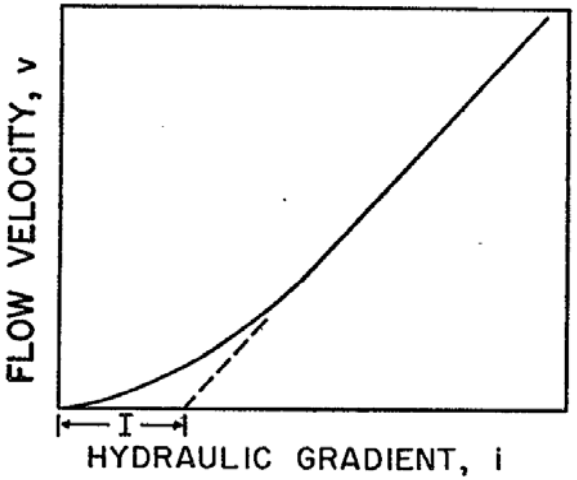

$$I = \frac{I*}{\alpha}\gamma\left(\frac{1}{\alpha}\right) \qquad \gamma(a,x) = \int_0^x t^{a-1}e^{-t}dt \qquad \gamma(a) = \int_0^\infty t^{a-1}e^{-t}dt$$

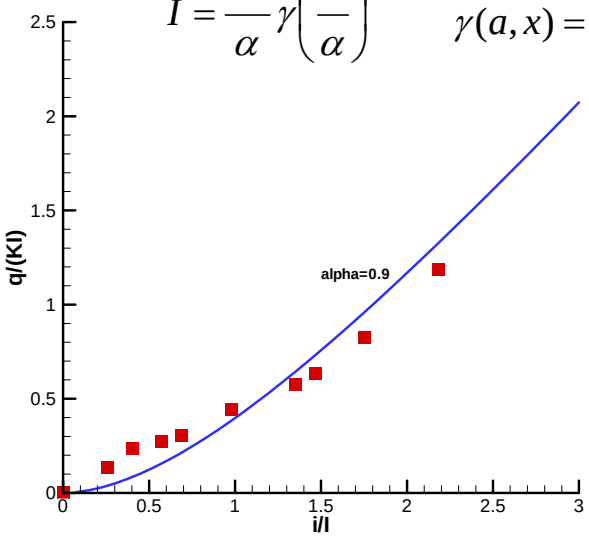

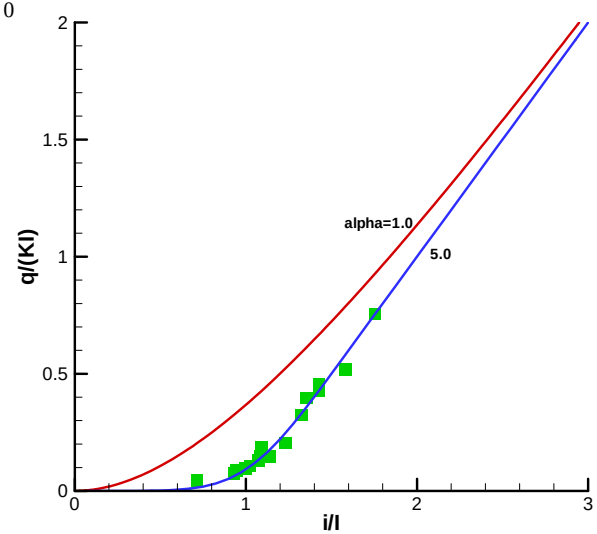

Relationship between permeability and threshold hydraulic gradient

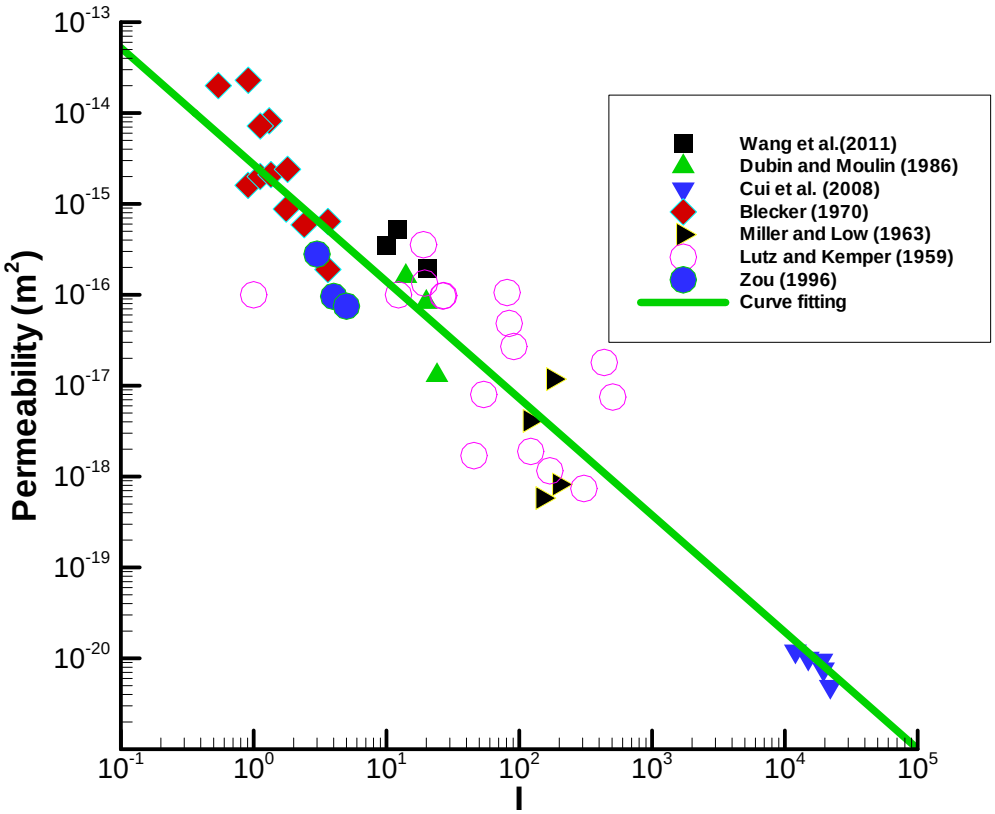

$$I = Ak^{B}$$

A= 4.0 E-12 and B =-0.78

Other Modeling Issues

- *Extension of the new flux-gradient relationship to multi-dimensions.*

$$\boldsymbol{q} = -K[i - \frac{I}{\gamma(\frac{1}{\alpha})}\gamma(\frac{1}{\alpha}, \left(\frac{i}{I*}\right)^{\alpha})]\boldsymbol{n_i}$$

- *The developed relationships can be applied to both saturated and unsaturated conditions.*
- *The impact of electrolyte concentration is partially considered through relationship between permeability and threshold gradient.*
- *The Current focus is on how to incorporate the temperature impacts.*

Used Fuel Disposition Campaign

Reactive Transport Processes in Clay and Clay-Rock

C.I. Steefel

J.A. Davis

R. Tinnacher

I.C. Bourg

J.M. Galindez

Earth Sciences Division

Lawrence Berkeley National Laboratory

Schematics of Electrical Double Layer

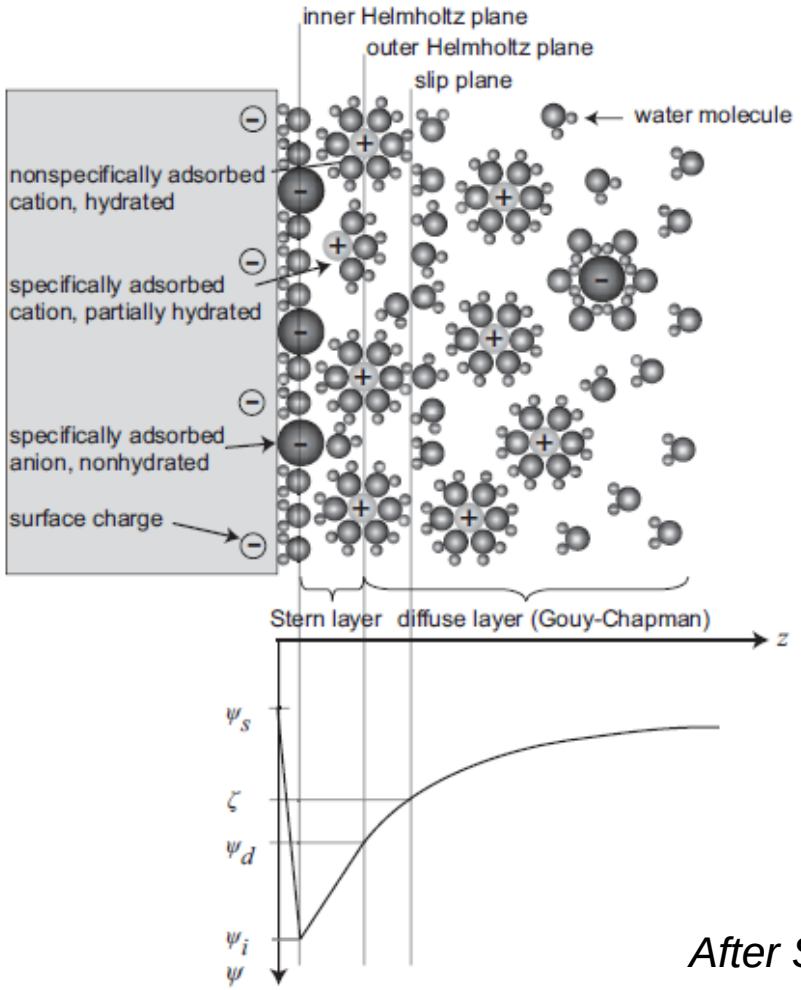

Double Layers between Charged Surfaces

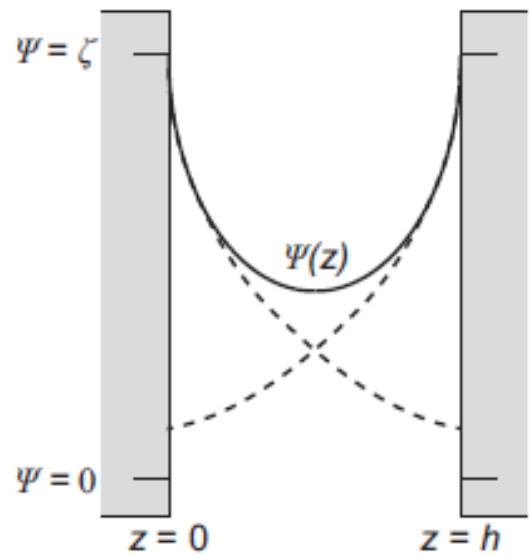

Solid line: Overlapping double layers
Dashed line: No opposite wall present

After Schoch et al, 2008

Mean Electrostatic (or Donnan) Potential Approach to Transport in Compacted Clay

Concentration in diffuse layer (DL) related to concentrations in bulk water (B) through the mean electrical potential, φ_m, of the diffuse layer

$$C_i^{DL} = C_i^B \exp\left(\frac{-z_i e \varphi_m}{k_B T}\right)$$

$$\phi^{DL} \sum_i z_i C_i^{DL} = Q^{SL} = \sum_k^{Ns} z_k \Gamma_k$$

Charge Balance Equation

Dynamic model for electrical double layer thickness as a function of ionic strength

$$\frac{\partial\left[\phi^B C_i^B + \phi^{EDL} C_i^{EDL}\right]}{\partial t} = \frac{\partial\left[\phi^B C_i^B + \left(A_{clay}\lambda_{DL}\beta_{DL} \big/ \sqrt{I}\right) C_i^{EDL}\right]}{\partial t}$$

Higher ionic strength front diffuses through clay, reducing EDL porosity, increasing bulk porosity

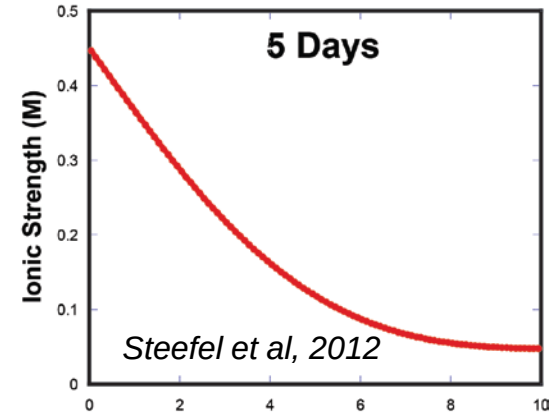

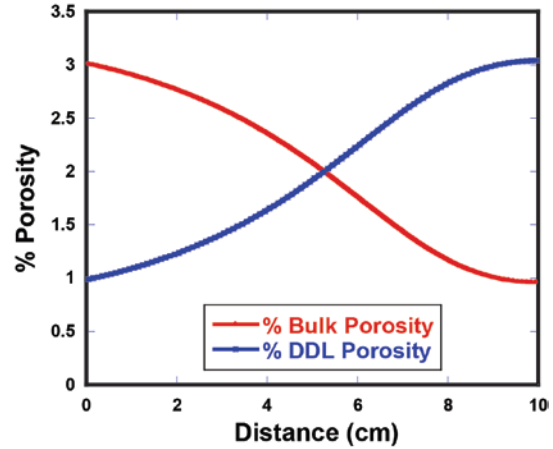

Recent improvements to model

- **Added ability to calculate double layer volume based on Debye length dynamically computed from ionic strength**
- **Developed model for inner sphere sorption of cations (no H^+) balanced by electrical double layer**

Poisson-Nernst-Planck Description of Transport through Compacted Clay

- **Improved description of transport and electrical double layer is offered by solving the full Poisson-Boltzmann equation**

$$\frac{\partial^2 \varphi}{\partial x^2} = \frac{-e}{\varepsilon} \sum_i z_i C_i \exp\left(\frac{-z_i e \varphi(x)}{k_B T} \right)$$

Two-dimensional cation transport between charged clay surfaces simulated with Poisson-Boltzmann Equation

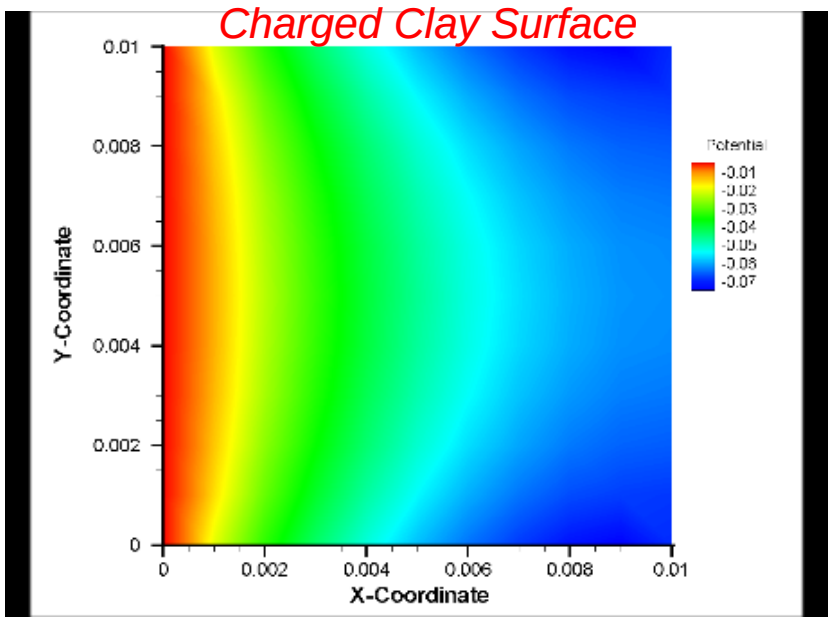

Ion Adsorption and Diffusion in Clay Barriers: Pore-scale studies

We determined the influence of simulation cell size, clay structural relaxation, and interlayer water content on molecular dynamics (MD) simulation results:

- Development of a robust methodology for simulating clay interlayer nanopores at a range of temperatures.
- Simulation results are consistent with experimental data showing that Na^+ has a lower activation energy of diffusion in the 3-layer hydrate of Na-montmorillonite than in bulk liquid water (Kozaki et al., 2005).

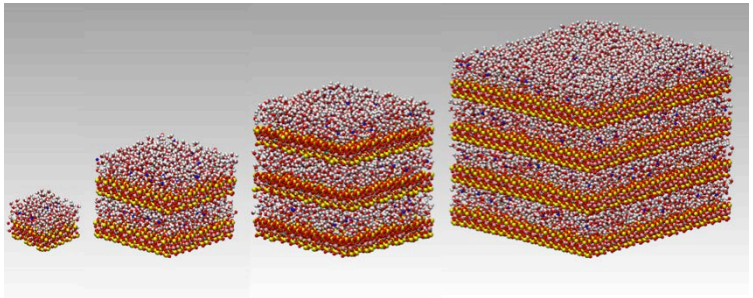

Simulation cells containing 1.3k to 136k atoms were used to test the influence of simulation cell size on predicted diffusion coefficients in Na-montmorillonite interlayer nanopores.

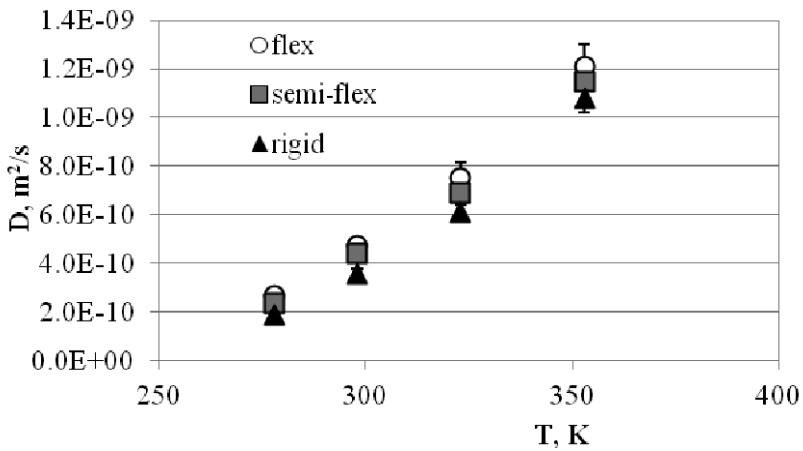

Diffusion in clay interlayers (and its temperature dependence) is sensitive to simulation choices such as the flexibility of the clay sheet.

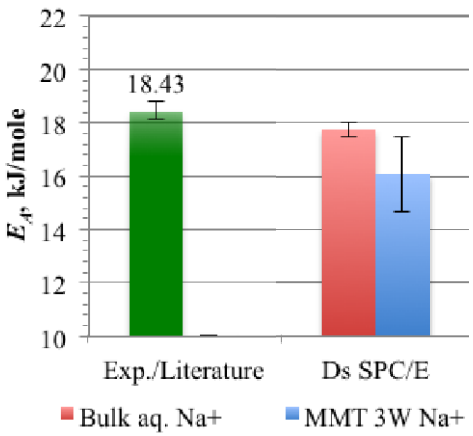

Activation energy of Na^+ diffusion (E_A):

- ***MD simulations of bulk liquid water (red) are consistent with experimental data (green),***
- ***the predicted E_A value in the 3-layer hydrate of Na-montmorillonite (blue) is lower than in bulk liquid water (red).***

Mont Terri DR-A Test

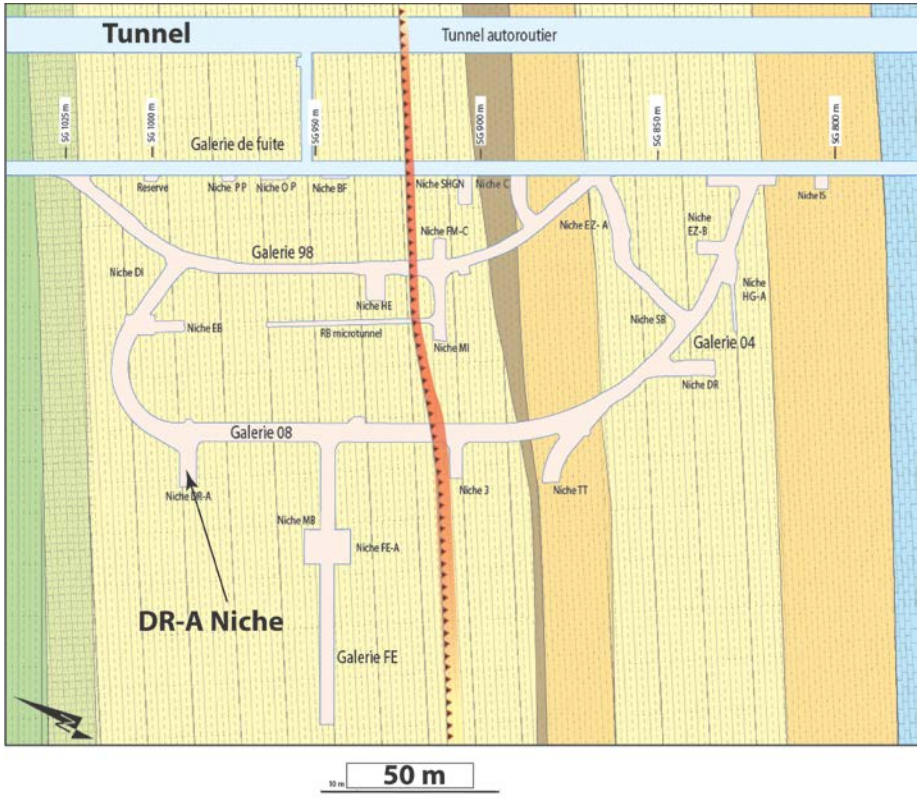

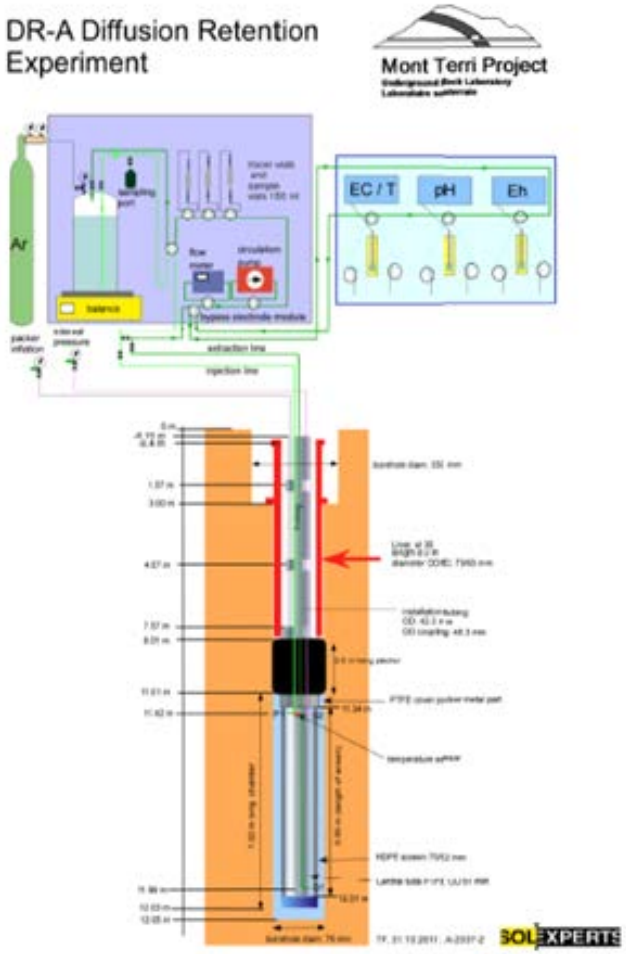

Figure 7: Schematic drawing of the entire test setup

Completed Test Problems from DR-A, Mont Terri

Test Problem 1: Non-Reactive Tracer

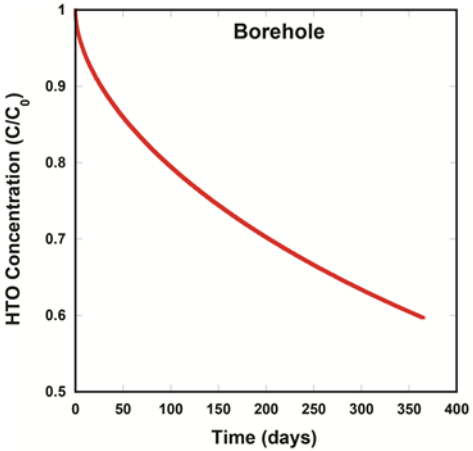

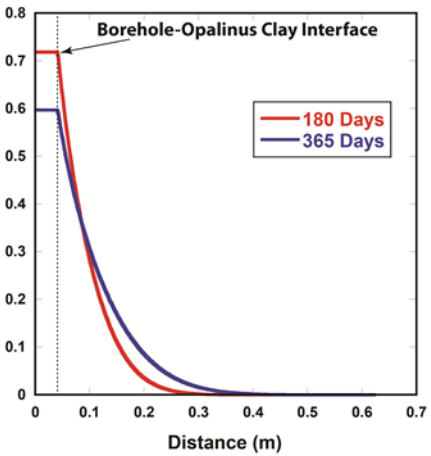

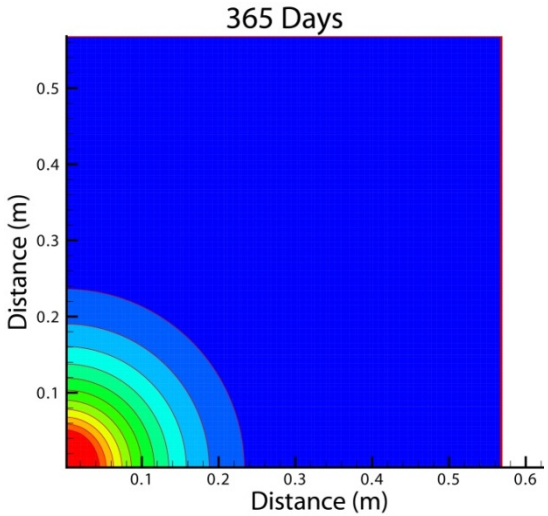

Test Problem 2:
Effect of Kd on Cs+ Transport

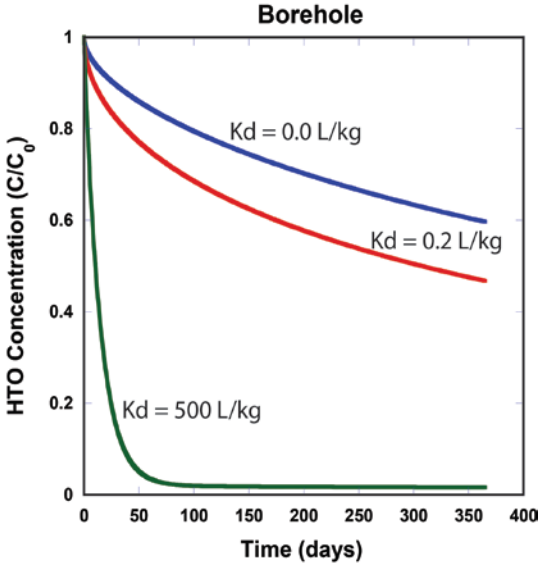

Test problems are part of the suite agreed upon by International Consortium modeling DR-A test

Conceptual Model

- **Cesium sorbs to multi-site cation exchange sites**
  - Edge sites with no treatment of EDL
- **Separate calculation of surface complexation on illite, with explicit treatment of EDL balancing fixed mineral+Stern layer charge**
  - Assumed 20% illite with 5×10^{-7} sites/m^2 and 200 m^2/g
- **EDL porosity determined by multiples of Debye length and total illite surface area**
  - Debye thickness depends on ionic strength
  - 1 Debye length → 1.1% EDL porosity, so 14% bulk porosity

(More or Less) Blind Simulation of Tracer

$D_p = 2.7 \times 10^{-10}\ m^2/s$
$D_e = 4.0 \times 10^{-11}\ m^2/s$

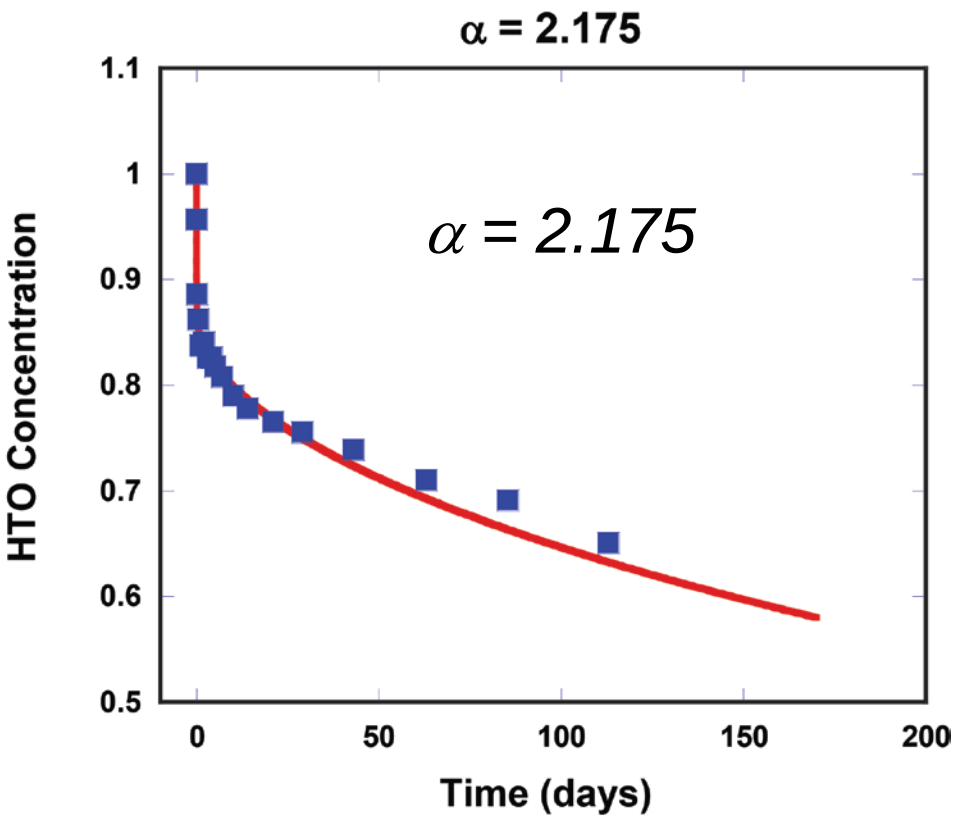

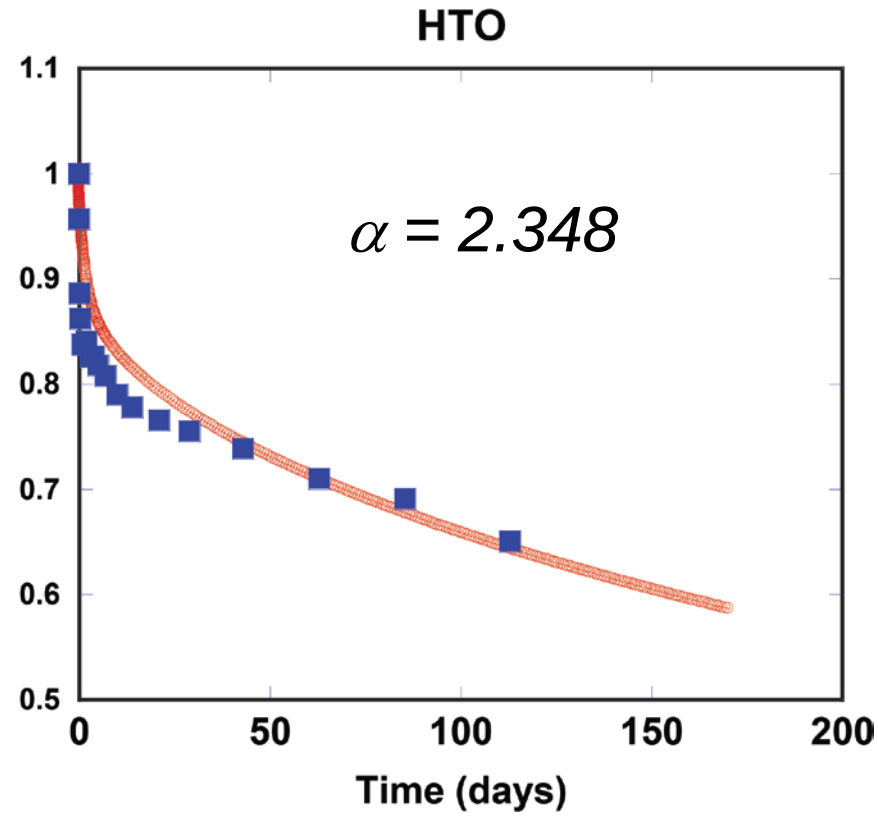

$De_filter = 1.2 \times 10^{-10}\ m^2/s$

Blind Simulation of Anions

20 wt % illite with sorption density of 5.88 x 10^{-7} mol/m^2 and specific surface area of 200 m^2/g

Total porosity: 15%
DDL porosity: 1.1%

Diffusion coefficients for anions in DDL porosity one order of magnitude less than tracer

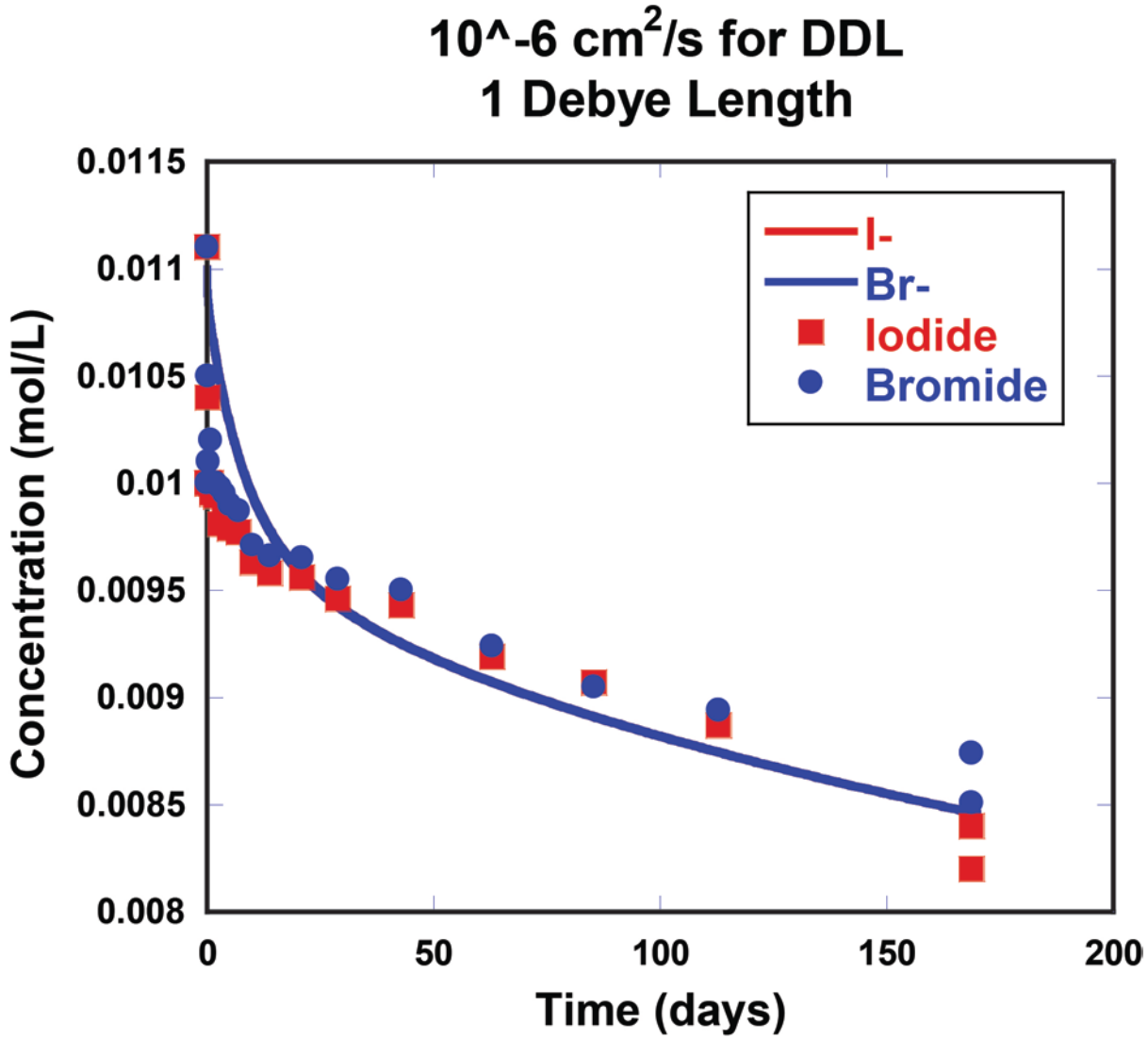

Comparison of Anion Diffusion Coefficients in DDL

High diffusion coefficient for filter

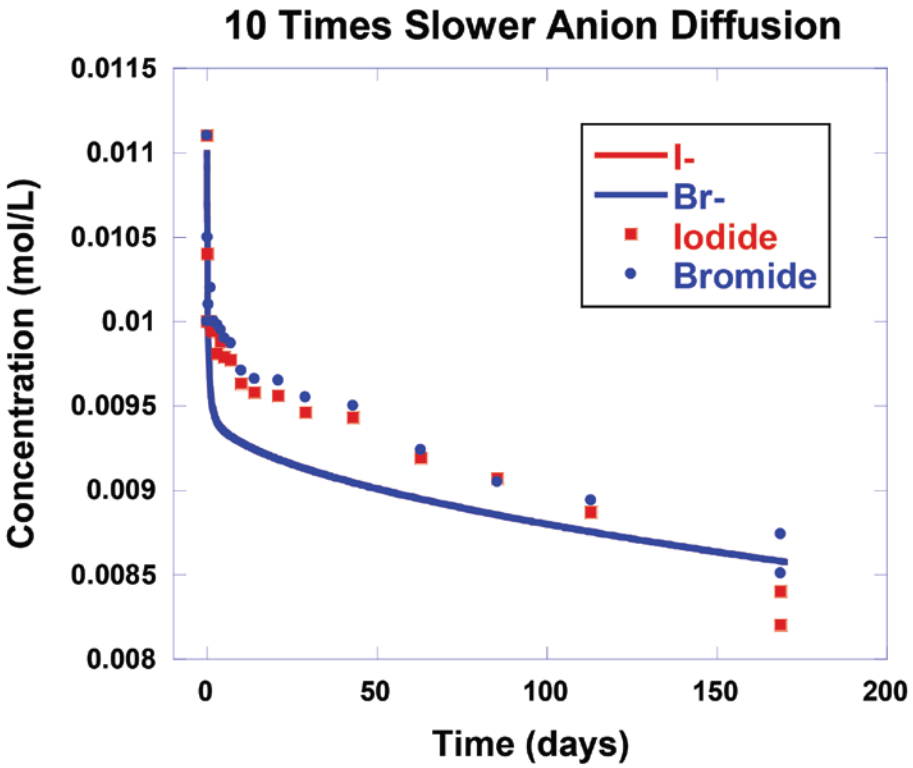

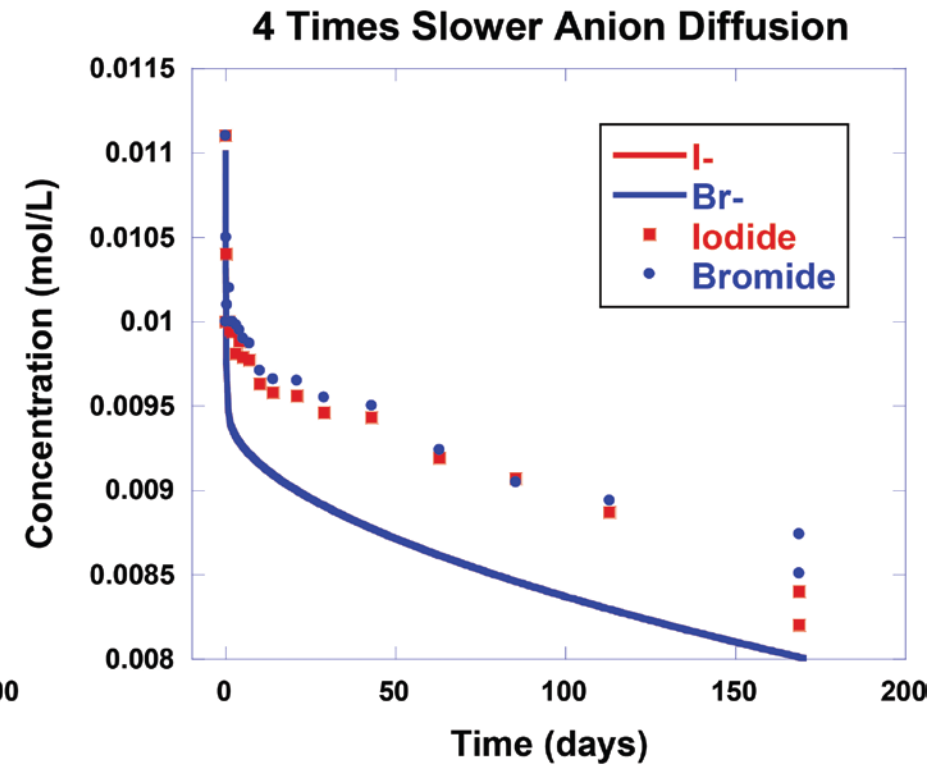

Modeling Opalinus Clay

- **Best fit for anion data using 8% porosity instead of 15%**

- **To simulate 8% anion accessible porosity requires a high clay surface area AND multiple Debye lengths**
  - Implication is that the pore size distribution in the Opalinus Clay is such that pore throats lined with clay exclude substantially larger portions of the overall connected pore network

Uranium(VI) Diffusion Experiments: Introduction

- **Research motivation and goals**
  - **Uranium(VI) solution speciation can affect uranium diffusion rates into bentonite due to differences in charge and sorption properties of various U(VI) species.**
  - **Important to de-couple the effects of solution speciation on sorption and diffusion processes to increase the 'predictive power' of apparent diffusion coefficients under varying chemical conditions.**
  - **Characterize U(VI) sorption and diffusion behavior in terms of chemical conditions (pH, ionic strength, salt composition and carbonate concentration) and degree of clay compaction.**

- **Research approach**
  - **Lab-scale experiments to evaluate U(VI) sorption and diffusion behavior.**
  - **Collaboration with Carl Steefel and Ian Bourg (LBNL) on development of a reactive U(VI) diffusion model.**

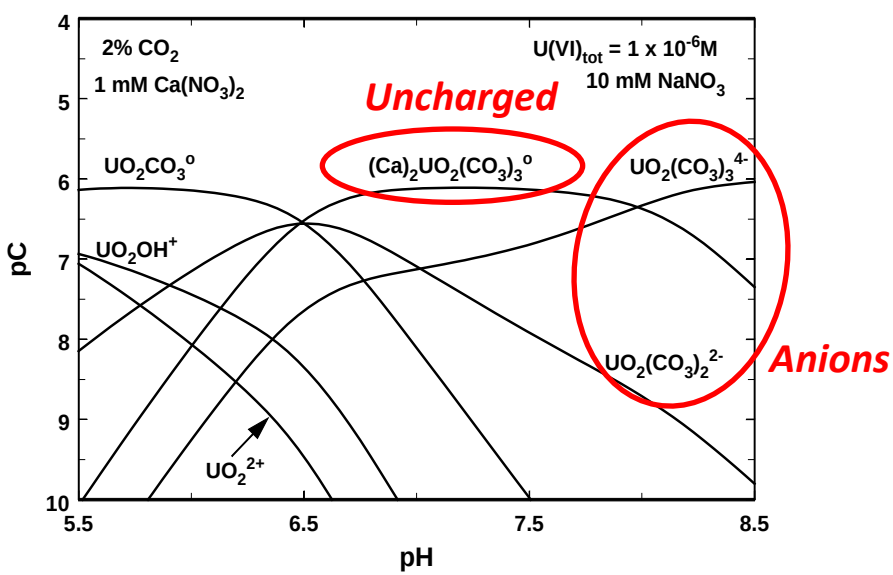

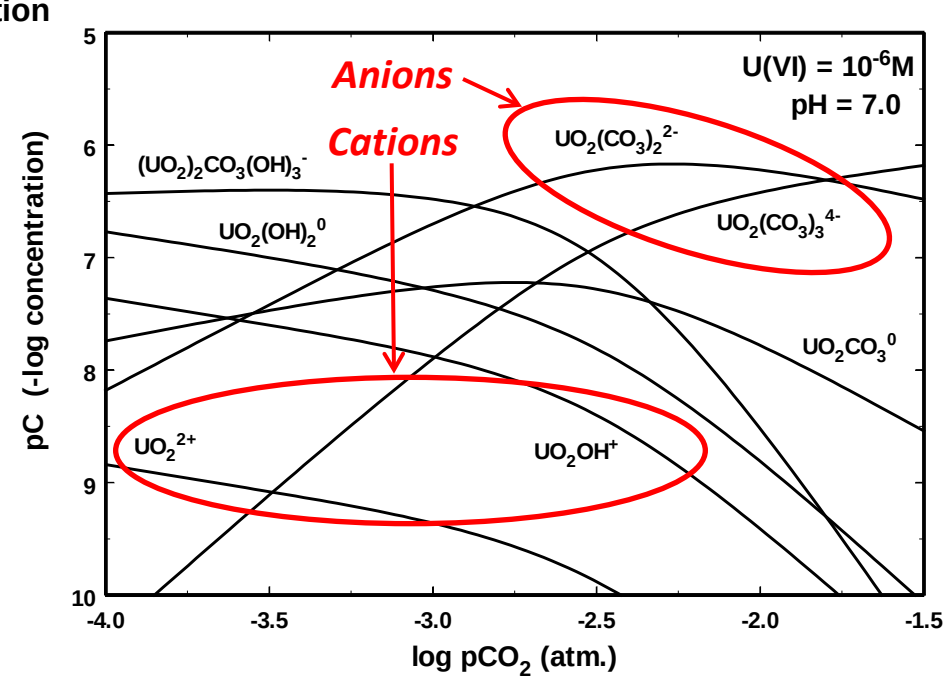

U(VI) Sorption and K_d Values

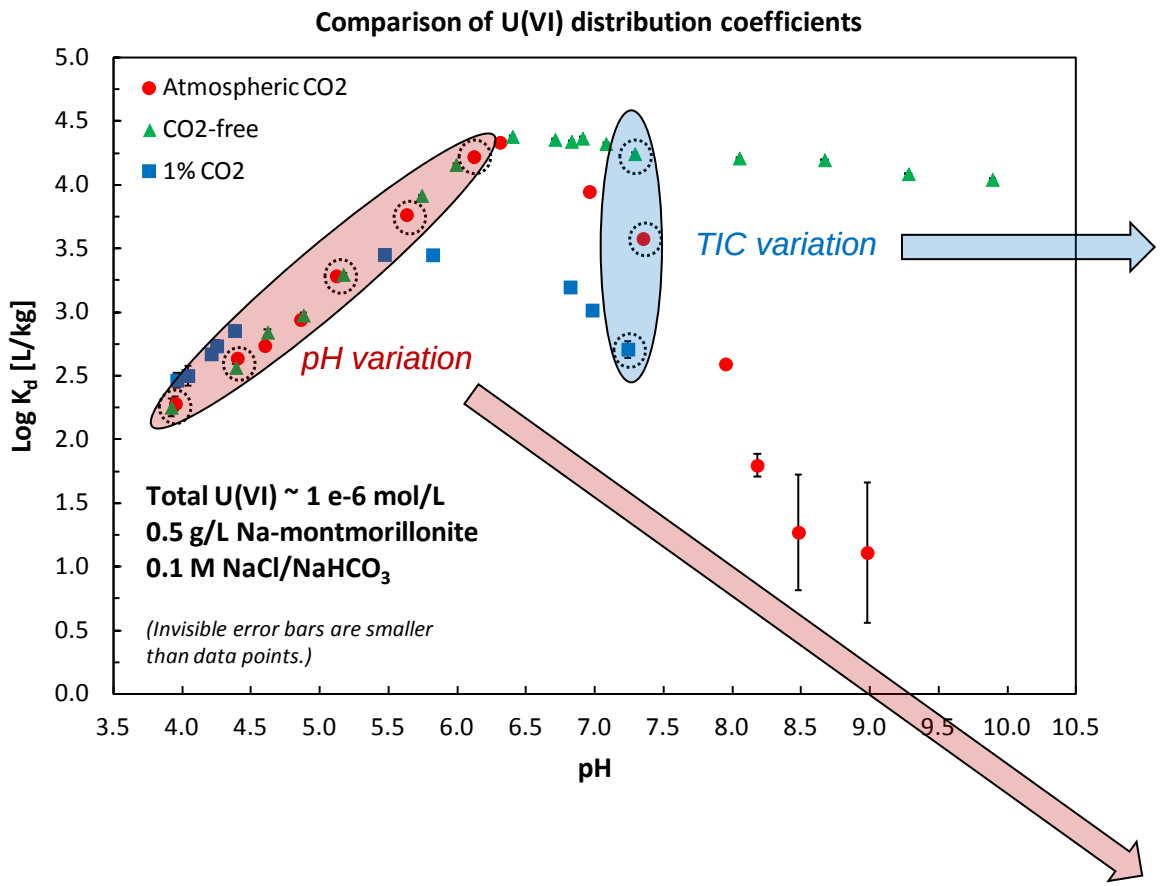

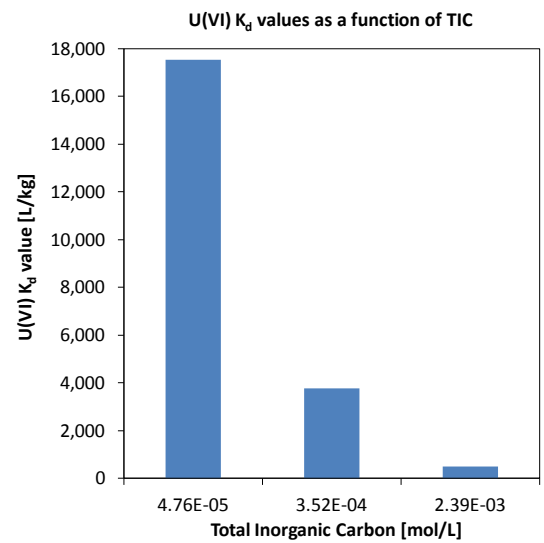

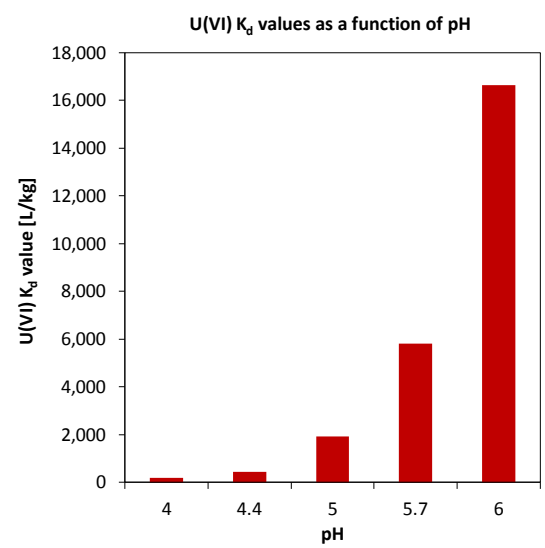

Diffusion of U(VI) in montmorillonite

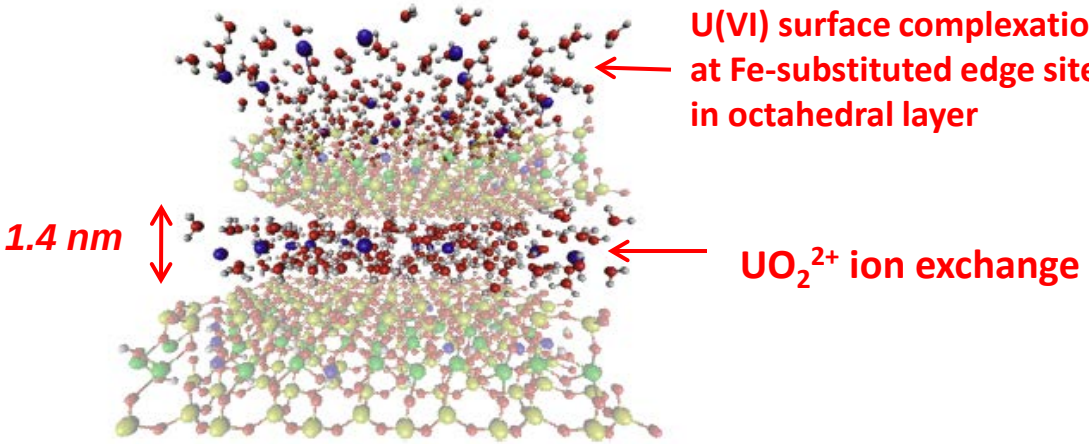

Two-layer hydrate of Na-montmorillonite, the predominant mineral phase in compacted bentonite, with Na (blue), water O (red), and water H (white) atoms in the interlayer and Si (yellow), Al (green), Mg (blue), O (red), and H (white) atoms (Bourg and Sposito, 2010).

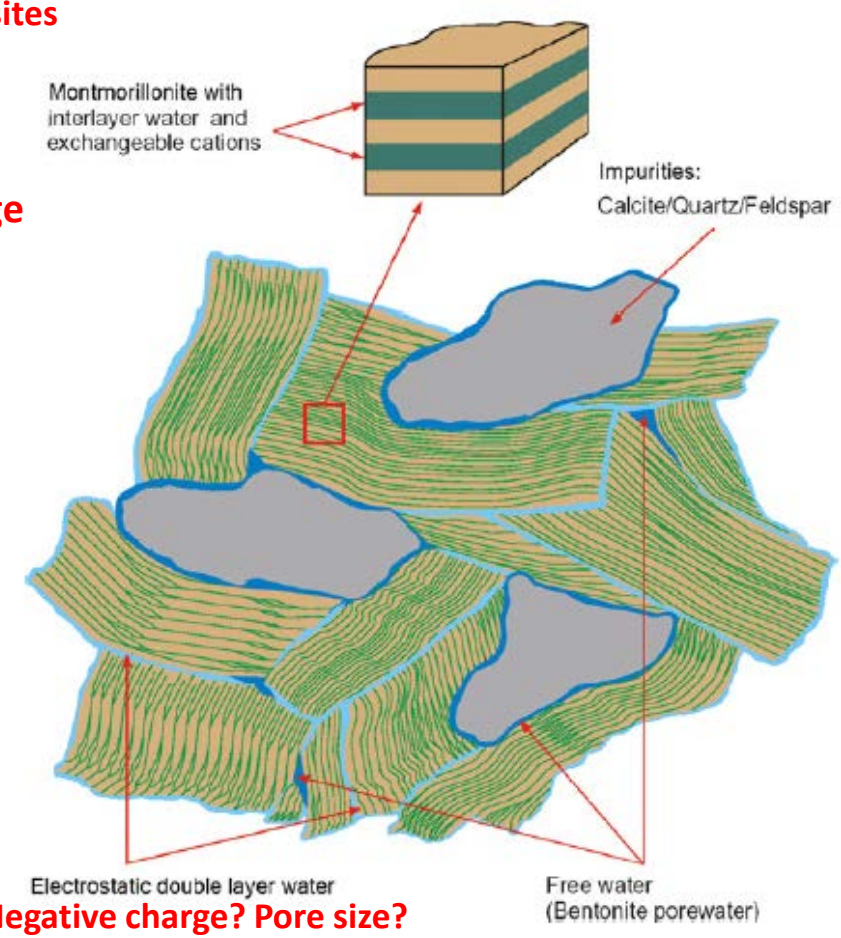

Schematic representation of interlayer water, electrostatic double layer water, and free water in compacted bentonite (Tournassat and Appelo, 2011).

Experimental observations on diffusion:

1. **Upon compaction, anions do not enter the interlayer water regime, which makes up 99% of the water.**
2. **Cations and neutral species, if small enough, may diffuse in the interlayer water regime. Cation diffusion may be retarded by sorption.**

Classical Diffusion Laws

<u>Fick's first law (steady-state flux):</u> $J = -D_e(dC/dx)$, where J is the solute flux, D_e is the "effective" diffusion coefficient, and dC/dx is the concentration gradient, and $D_e = D_o(\delta/\tau^2)\omega$, where D_o is the molecular diffusion coefficient in water, ω is the total porosity, δ is a constrictivity factor, and τ is a tortuosity factor.

<u>Ficks's second law (flux time dependence)</u>: $dC/dt = D_a(\delta^2C/\delta x^2)$ where C is solute concentration and $D_a = D_e/(\omega + \rho K_d)$, where D_a is the "apparent" diffusion coefficient, ρ is the clay density, and K_d is a sorption partitioning coefficient.

- **<u>Goal:</u>**
  - **Predict U(VI) diffusion profiles as a function of pH and total inorganic carbon (TIC) in a lab-scale diffusion cell.**

- **<u>Approach:</u>**
  - **Replace K_d value with a more robust surface complexation model that is predictive for U(VI) diffusion under variable U(VI) speciation and accounts separately for U(VI) binding to edge sites and ion exchange sites.**

Diffusion cell design

- **Characteristics of through diffusion experiments:**
  - **At beginning of experiment:**
    - **Constant U(VI) concentration in inlet solution**
    - **No U(VI) in collection reservoir (outlet solt.)**
  - **During experiment:**
    - **Continuous monitoring of U(VI) solution concentrations in inlet and outlet solutions**
    - **Goal: Constant U(VI) conc. in inlet solution**
  - **At the end of experiment:**
    - **Preparation of ~20-100 µm clay slices with 'soil abrasion technique'** ***(Van Loon & Eikenberg, 2005)***
    - **U(VI) desorption from individual clay slices and analysis of total U(VI) concentrations**
    - **If feasible:**
      Analysis of U(VI) conc. in pore solutions

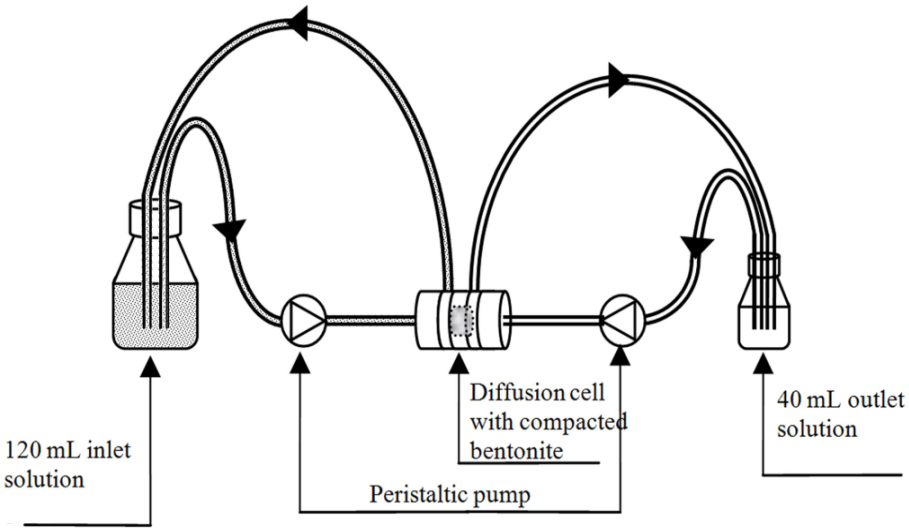

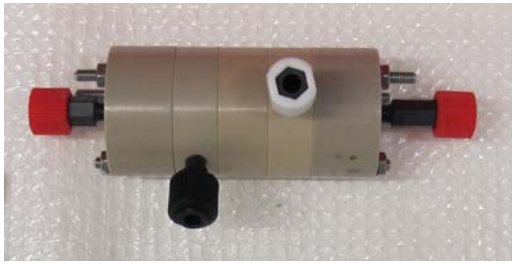

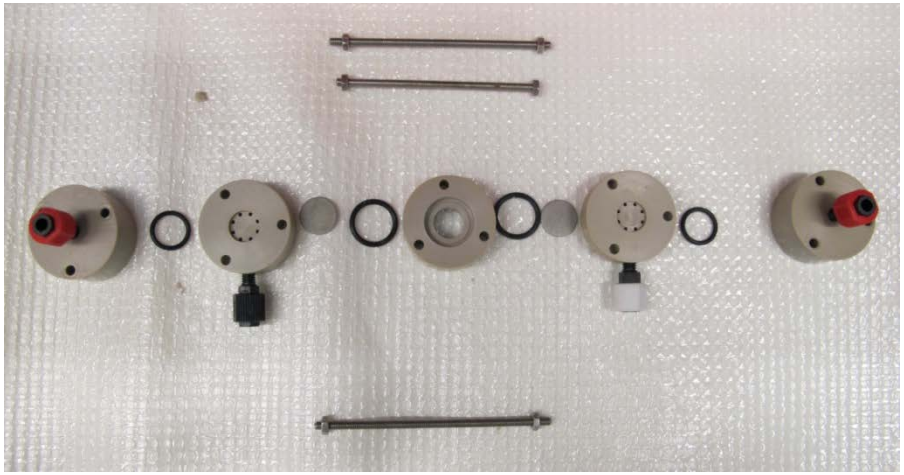

Pictures: Courtesy of Michael Holmboe

Preliminary Diffusion Modeling

Lab-scale through diffusion experiments

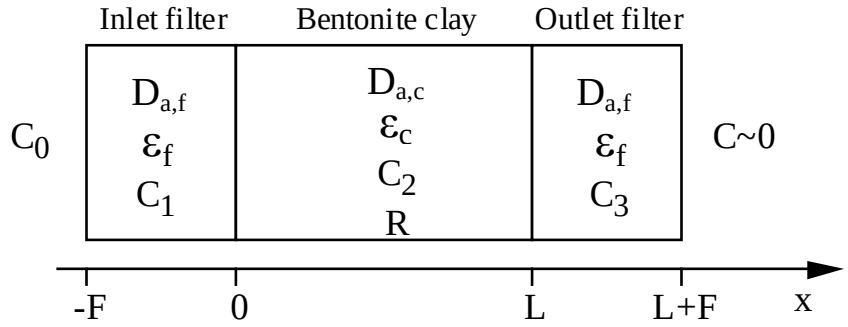

Schematic representation of diffusion cell. Clay is sandwiched between two filter plates.

Fixed input parameters

	Parameter	Value (units)
Filters	Thickness	0.155 (cm)[1)]
	Porosity	0.3 (-)[1)]
	Cross-sectional area	5.11 (cm^2)[1)]
Clay packing	Length	1.1 (cm)[1)]
	Porosity	0.512 (-)[2)]
	Dry density	1.4 (g/cm^3)[2)]
	Cross-sectional area	5.11 (cm^2)[1)]
Solutions	Conc. in source reservoir	10^{-6} (M)
	Conc. in receiving reservoir	0 (M)
Experiment	Time of interest	360 (days)

[1)] Van Loon et al., *J. Contam. Hydrol.* **2003,** *61*, (1-4), 73-83.
[2)] Korichi, et al., *Defect Diff. Forum* **2010,** *297-301*, 275-280.

Variable input parameters: $D_{a,f}$, $D_{a,c}$, K_d

Sim.	pH	CO_2	TIC	Dominant U(VI) species	D_0 [1)]	$D_{e,f}$	$D_{a,f}$ [2)]	$D_{a,c}$	K_d
( )	( )	( )	(mol/L)	( )	(m^2/sec)	(m^2/sec)	(m^2/sec)	(m^2/sec)	(L/kg)
Variable TIC, comparable pH conditions (pH~7.3)									
1	7.29	'CO_2-free'	4.76E-05	$(UO_2)_2CO_3(OH)_3^-$	6.10E-10	6.10E-11	2.03E-10	8.60E-13	17,528
2	7.35	Atm. CO_2	3.52E-04	$(UO_2)_2CO_3(OH)_3^-$	6.10E-10	6.10E-11	2.03E-10	3.99E-12	3,780
3	7.24	1% CO_2	2.39E-03	$UO_2(CO_3)_2^{2-}$	5.52E-10	5.52E-11	1.84E-10	2.94E-11	512
Variable pH, comparable TIC concentrations (TIC~2E-05 mol/L, atmospheric CO_2)									
4	3.95	Atm. CO_2	1.10E-05	UO_2^{2+}	7.66E-10	7.66E-11	2.55E-10	7.88E-11	191
5	4.40	Atm. CO_2	9.45E-06	UO_2^{2+}	7.66E-10	7.66E-11	2.55E-10	3.47E-11	434
6	5.12	Atm. CO_2	2.18E-05	UO_2^{2+}	7.66E-10	7.66E-11	2.55E-10	7.83E-12	1,925
7	5.63	Atm. CO_2	2.88E-05	$UO_2(OH)^+$	7.66E-10	7.66E-11	2.55E-10	2.59E-12	5,820
8	6.12	Atm. CO_2	5.12E-05	$UO_2(OH)^+$	7.66E-10	7.66E-11	2.55E-10	9.06E-13	16,624

[1)] From Kerisit & Liu, *Geochim. Cosmochim. Acta* **2010,** *74*, (17), 4937-4952 and Kerisit, personal communication; [2)] Assuming a filter porosity of 0.3 (-)

ANADIFF Reference: **TR-96-16, Eriksen & Jansson, SKB Techn. Report, 1996.**

Diffusion Modeling Results

- **Diffusion profiles: Variable Total Inorganic Carbon, similar pH** ***(Total uranium(VI) conc.)***

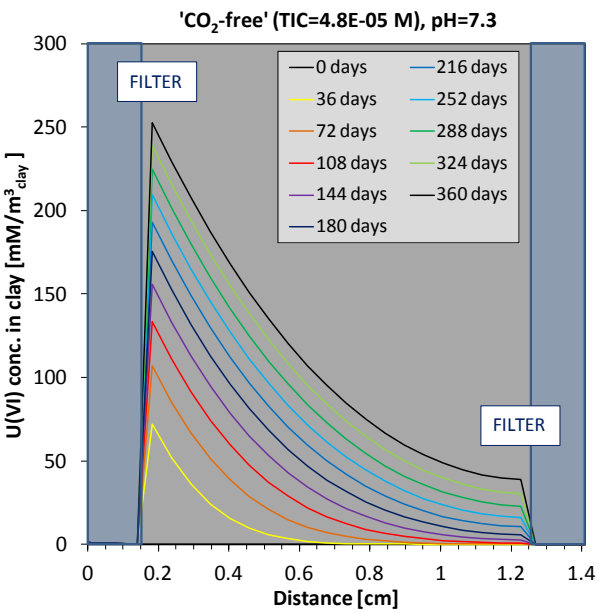

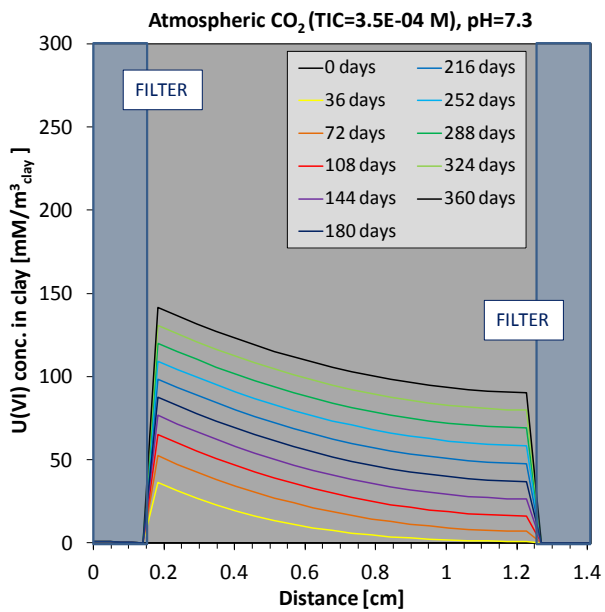

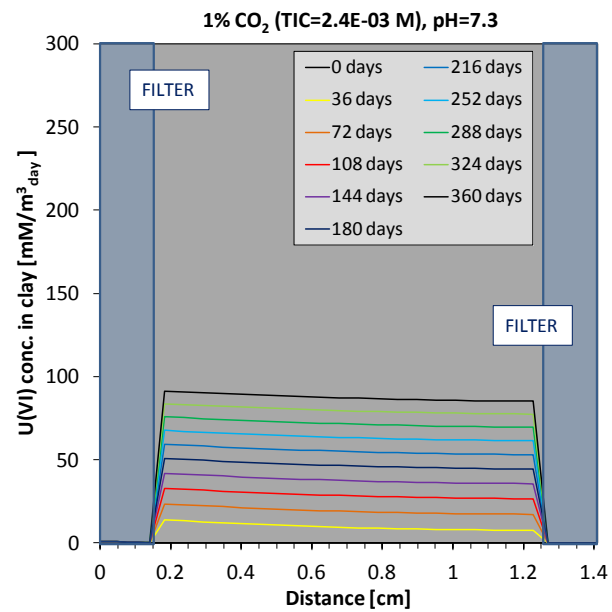

Increase in Total Inorganic Carbon (TIC)

U(VI) Sorption and K_d Values

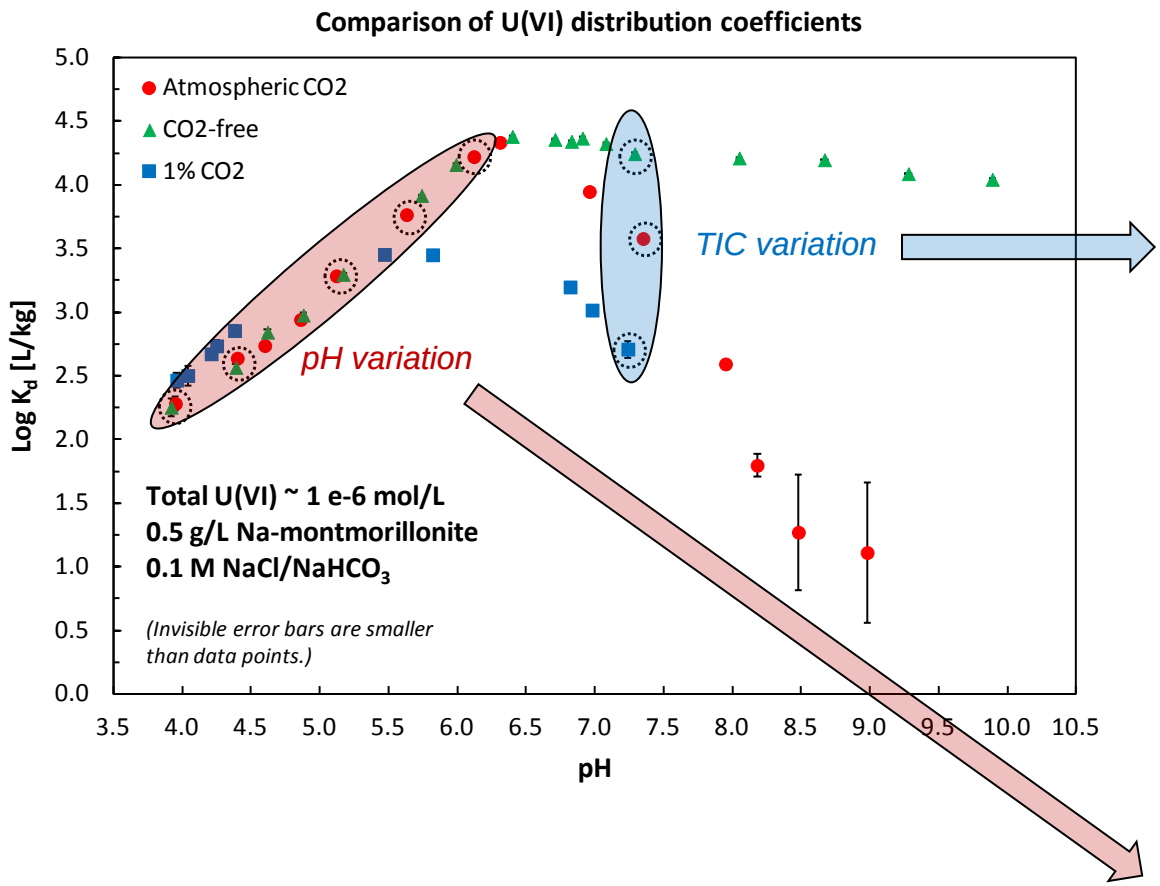

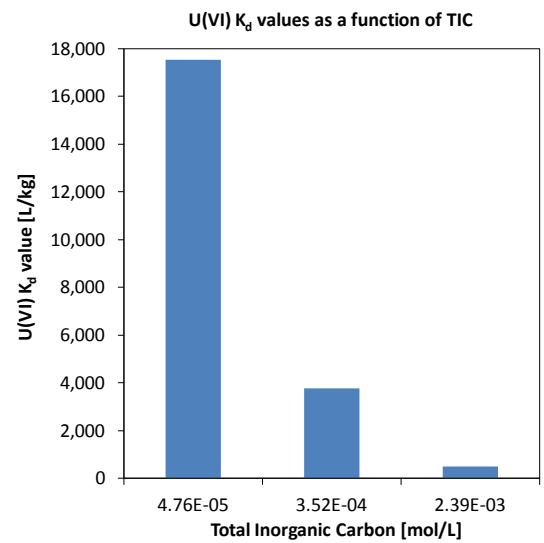

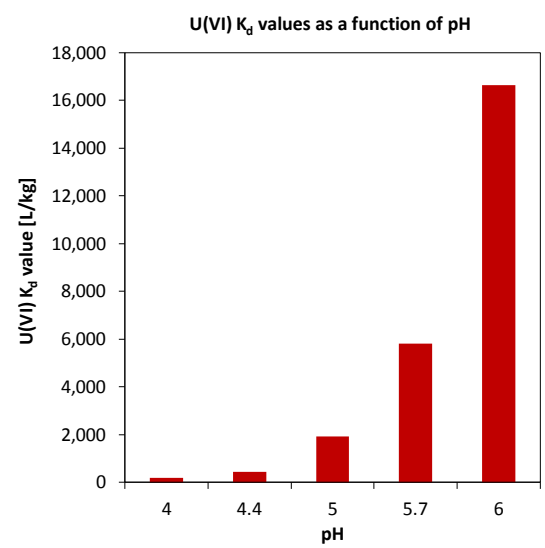

Diffusion Modeling Results

- **Diffusion profiles: Variable pH, similar Total Inorganic Carbon** ***(Total uranium(VI) conc.)***

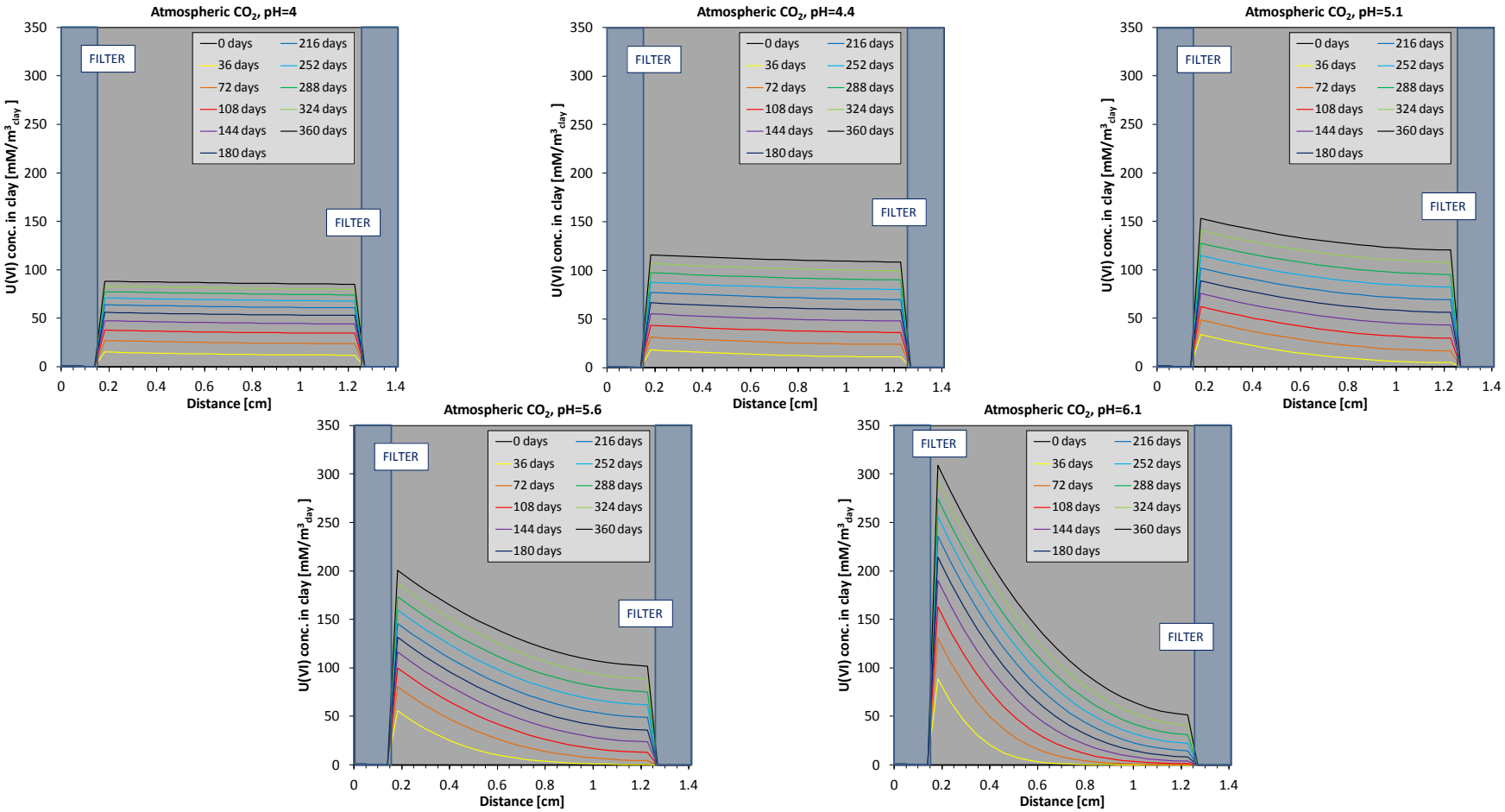

Increase in pH

RN Diffusion Experiments: FY 2013 Work Plan

- **Uranium sorption studies: Experimental and modeling**
  - **Conduct kinetic and equilibrium U(VI) sorption experiments on montmorillonite as a function of calcium concentration.**
  - **Conduct batch kinetic and equilibrium U(VI) sorption experiments on montmorillonite as a function of temperature.**
  - **Complete/refine the surface complexation model for U(VI) sorption on montmorillonite by incorporating all experimental data.**

- **Uranium diffusion studies: Experimental and modeling**
  - **Conduct study of Br^- and Ca^{2+} diffusion into montmorillonite at low compaction and at pH 7 in 0.1M NaCl solutions equilibrated with air.**
  - **Conduct studies of U(VI) diffusion into montmorillonite at low compaction and**
    - **at low pH (5.0),**
    - **circumneutral pH (7.0) and**
    - **high pH (8.5)**

    in 0.1M NaCl solutions equilibrated with air.
  - **Conduct study of U(VI) diffusion into montmorillonite at low compaction at pH 7 in 0.1M NaCl/1 mM $CaCl_2$ solution equilibrated with air.**
  - **Conduct study of U(VI) diffusion into montmorillonite at intermediate and high compaction at pH 7 in 0.1M NaCl/1 mM $CaCl_2$ solution equilibrated with air.**
  - **Conduct study of montmorillonite porosity distribution and type as a function of compaction using SANS in collaboration with Mei Ding (LANL).**
  - **Modeling collaboration with Carl Steefel and Ian Bourg (LBNL) on development of a reactive U(VI) diffusion model.**

Areas/ideas for collaboration??

- **Porosity distribution and type in compacted clay?**
- **Compacting methods?**
- **Diffusion cell design?**
  - **Later adaptation?**
- **Liquid phase sampling within compacted clay?**